DISTRIBUTION STATEMENT A
Approved for public release
Distribution Unlimited

DTIC QUALITY INSPECTED 4

19980408 128

DEPARTMENT OF THE AIR FORCE

AIR UNIVERSITY

AIR FORCE INSTITUTE OF TECHNOLOGY

Wright-Patterson Air Force Base, Ohio

AFIT/GM/ENP/98M-10

A VALIDATION STUDY OF THE AIR FORCE WEATHER AGENCY (AFWA) JETRAX CONTRAIL FORECAST ALGORITHM

THESIS

Jeffrey D. Shull, Captain, USAF

AFIT/GM/ENP/98M-10

Approved for public release; distribution unlimited

The views expressed in this thesis are those of the author and do not reflect the official policy or position of the Department of Defense or the U. S. Government.

AFIT/GM/ENP/98M-10

A VALIDATION STUDY OF THE AIR FORCE WEATHER AGENCY (AFWA) JETRAX CONTRAIL FORECAST ALGORITHM

THESIS

Presented to the Faculty of the Graduate School of Engineering

of the Air Force Institute of Technology

Air University

Air Education and Training Command

In Partial Fulfillment of the Requirements for the

Degree of Master of Science in Meteorology

Jeffrey D. Shull

Captain, USAF

March, 1998

Approved for public release; distribution unlimited

AFIT/GM/ENP/98M-10

A VALIDATION STUDY OF THE AIR FORCE WEATHER AGENCY (AFWA) JETRAX CONTRAIL FORECAST ALGORITHM

Jeffrey D. Shull, B.S.
Captain, USAF

Approved:

Michael K. Walters, Lt Col, USAF
Chairman, Advisory Committee

6 MAR 98
Date

Paul J. Wolf, Lt Col, USAF
Member, Advisory Committee

6 MAR 98
Date

Clifton E. Dungey, Maj, USAF
Member, Advisory Committee

6 MAR 98
Date

Daniel E. Reynolds
Member, Advisory Committee

6 March 98
Date

Acknowledgments

I would like to thank my thesis advisor, Lieutenant Colonel Michael K. Walters, for his guidance throughout the entire thesis process. From selecting and narrowing a viable topic to the final presentation, his enthusiasm for the subject matter and genuine interest in my progress provided me with both motivation and confidence to see this project through. I wish to recognize all the members of my advisory committee for their assistance during my research and writing efforts, but particularly for their outstanding instruction during the course work I completed while at AFIT. What I've learned from Lieutenant Colonel Walters' Atmospheric Dynamics courses, the Atmospheric Physics class taught by Major Cliff Dungey, and Mr. Dan Reynolds' Statistics classes provided me with a solid background that served me well throughout the writing of this thesis and will continue to do so throughout my Air Force career.

I would be remiss not to express my thanks to Captain Rob Asbury for writing such an outstanding thesis on a similar subject last year. He established the basis for the observation method I used during my research, wrote one of the major computer algorithms I used to analyze my observation data, and wrote a thorough report which provided the framework for my own. I will be the first to admit that my job was made much easier by the fact that I had such an excellent product to emulate.

Along those same lines, I would like to thank the members of the 88th Weather Squadron here at Wright-Patterson Air Force Base. They provided me the same outstanding assistance and expertise that they provided to Captain Asbury last year, and

were truly instrumental in the success of both of our research efforts. In particular I would like to recognize:

Major Mike Kapel, who brought in his own 8mm tape player from home so I could analyze the aircraft observations I recorded on video;

Captain John Polander, who modified several DOS programs to help better analyze upper air sounding data;

Captain Andy Goodnite, who provided valuable computer support including helping me recover from an inopportune hard drive crash;

Captain Jim O'Connor, who conducted a radiosonde data comparison with three different soundings, giving me great confidence in the Vaisala sondes I used;

and I would especially like to thank Mr. Steve Weaver for his help in consolidating a great deal of relevant literature and for providing insightful feedback once the writing phase began. Thanks again to everyone in the 88th for all of their help.

I would like to thank Master Sergeant Israel Laracuente of the Weather Displays and Applications Branch of the organization then known as the Air Force Global Weather Center for providing me a wealth of background information on the JETRAX contrail forecast model. He went out of his way to send me the JETRAX code via electronic mail and patiently answered my questions over the telephone. I am grateful for his assistance. I would also like to express my appreciation to my good friends and AFIT classmates Captain Brian Pukall, Captain Tony Eckel, and Lieutenant Jon Thompson for helping me with the Microsoft issues that came up as I tried to present my results in a legible form and for providing critically important statistical assistance.

There are numerous individuals and organizations outside of the Air Force Weather community to whom I would like to express my appreciation as well. I would like to thank Colonel John Kent, Major John Andreano, Technical Sergeant Wiley Wells, and Mr. Albert Chapin from the Fitts Human Engineering Division of Armstrong Laboratory here at Wright-Patterson. When I inquired about using their observation tower for taking contrail observations they were more than accommodating.

The use of the DBRITE radar scope in the air traffic control tower proved to be a major breakthrough for my data collection efforts, and for that opportunity I have to thank the Chief Controller at Wright-Patterson Air Force Base, Senior Master Sergeant DeEtte Slattery. She and all of the air traffic controllers under her supervision took the time to instruct me on the use of the DBRITE and the Flight Data System in the tower, permitting the collection of a much larger and more statistically significant data set than would have otherwise been possible. They are a highly professional group of people, and I would like to thank them each individually for their assistance in my research. By shift, they are:

A TEAM	B TEAM	C TEAM	D TEAM
TSgt Rob Tetrault	TSgt Scott Hayes	SSgt Brent Laird	SSgt Joe Weston
SSgt Mike Richmond	SrA Jay Fellers	SSgt Rodney Smith	SSgt Larry Morris
SSgt Troy Stempfley	A1C Jason Six	SSgt Steve Yantko	SSgt Eric Rogalinski
A1C Julie Neff		Amn Latisha Gray	TSgt Jim Duke

The attempt to verify the exact bases of the contrail layer could not have been possible without the cooperation of the 445th Airlift Wing of the Air Force Reserve and the 178th Fighter Group of the Ohio Air National Guard. Thank you to Colonel Tom Pape, the F-16 pilots, and the rest of the operations staff at the 178th for their part in helping me gain the low bypass aircraft observations I was looking for. Likewise, I'd like to thank Rob Fetner of the Air Force Research Laboratory at Wright Patterson for allowing me to fly with them during their airborne lidar testing, and to the C-141 crews of the 445th.

I would like to express my thanks to Mr. Orvin Shamblin, a civilian contractor working in AFIT/SC, who was somehow able to rescue most of the data files from a computer hard drive that crashed during the data collection phase of my research. He truly went above and beyond the call of duty to help me out, and I greatly appreciate his assistance. Thanks also to AFIT Resource Advisor Elaine Tabbert and Physics Lab Technician Greg Smith, who were very helpful in my helium acquisition efforts, and to Barbara Roddy at the FAA's Indianapolis Center for all the flight data she patiently compiled for me.

Each of the people above made a tangible contribution to the eventual success of this project, but I would like to conclude these lengthy acknowledgments by thanking those who provided invaluable moral support throughout the entire process. Thanks to my mom and dad who have always given me their unconditional support and encouragement in all of my endeavors, and to Cassandra and Zachary Shull, my two wonderful children, who are truly the light of my life. At six and five years of age, Casey and Zack were a little young to understand what this thesis was all about. They were patient with me

nonetheless, and they did enjoy the part about launching the weather balloons. The promise of their future continues to motivate everything I do. I would finally like to thank the Lord for so richly blessing my life. Particularly over the past couple years, there have certainly been times in our walk together where the only set of Footprints in the sand were His.

Jeffrey D. Shull

Table of Contents

Page

Acknowledgments iii

List of Figures xiii

List of Tables xiv

Abstract xvi

I. Introduction 1

1.1 Background 1

1.1.1 Definition of Contrails 1

1.1.2 Rationale for Contrail Forecast Verification 2

1.1.3 The Air Force Weather Agency JETRAX Contrail Forecast Model 3

1.2 Problem Statement 7

1.2.1 Primary Focus of This Research 7

1.2.2 Additional Objectives 8

1.3 The Benefit of Solving the Problem 9

1.4 Approach 10

1.4.1 Data Collection 10

1.4.2 JETRAX Validation 10

1.4.3 Algorithm Comparison 11

1.4.4 Exact Bases 11

1.5 Thesis Organization 12

Page

II. Literature Review 14

2.1 *The Formation of Exhaust Condensation Trails by Jet Aircraft*, Herbert Appleman, 1953 14

2.2 *A Further Analysis of Contrail Data*, Air Weather Service, 1953 23

2.3 *Derivation of Jet Aircraft Contrail Formation Curves*, Herbert Appleman, 1957 24

2.4 *Prediction of Aircraft Condensation Trails*, PROJECT CONTRAILS, James E. Jiusto, 1961 25

2.5 *Contrails Forecasting*, James E. Jiusto and Roland J. Pilie, 1964 28

2.6 *Forecasting Aircraft Condensation Trails*, Air Weather Service, 1981 29

2.7 *SAC Contrail Forecasting Algorithm Validation Study*, Walter F. Miller, 1990 29

2.8 *New Techniques for Contrail Forecasting*, Jeffrey L. Peters, 1993 30

2.9 *Calculations of Critical Temperature of Contrail Formation for Different Engine Types*, Mark L. Schrader, 1994 33

2.10 *A Reexamination of the Formation of Exhaust Condensation Trails by Jet Aircraft*, Harvey M. Hanson and Douglas M. Hanson, 1995 34

2.11 *Pilot Alert System Flight Test Final Report*, P. Saatzer, 1995 36

2.12 *Validation of the Appleman Contrail Forecasting Scheme Using Engine Specific Aircraft Data*, David J. Speltz, 1995 37

2.13 *On Conditions for Contrail Formation From Aircraft Exhausts*, Ulrich Schumann, 1996 38

2.14 *Comments on "A Reexamination of the Formation of Exhaust Condensation Trails by Jet Aircraft"*, Ulrich Schumann, 1996 39

2.15 *A New Formulation for the Critical Temperature for Contrail Formation*, Rich F. Coleman, 1996 40

Page

2.16 *SUbsonic aircraft: Contrail and Clouds Effects Special Study (SUCCESS)*, NASA, 1996 40

2.17 *A Diagnostic Study of the Global Coverage by Contrails*, Robert Sausen, Klaus Gierens, and Ulrich Schumann, 1997 42

2.18 *Surface Based Observations of Contrail Occurrence Frequency Over the U.S., April 1993-April 1994*, Patrick Minnis, J. Kirk Ayers, and Steven P. Weaver, 1997 43

2.19 *Contrail Cirrus and their Potential for Regional Climate Change*, Kenneth Sassen, 1997 44

2.20 *An Examination of the Hanson Contrail Forecast Algorithm Under Low Relative Humidity Conditions*, Robert P. Asbury III, 1997 44

2.21 *Moisture Sensitivity of Contrail Forecast Algorithms*, Allen C. Rabayda, 1997 45

III. Methodology 47

3.1 Data Collection 47

3.1.1 Ground Based Contrail Observations 47

3.1.1.1 Radiosonde Launches 48

3.1.1.2 Observation of Aircraft 50

3.1.2 Airborne Contrail Observations 53

3.2 Theory 55

3.2.1 Mixing Cloud Theory 55

3.2.2 Forecasting Contrail Formation 59

3.2.3 Critical Temperature Formulations 62

3.2.3.1 Schumann Method 63

3.2.3.2 Hanson Method 64

Page

3.2.3.3 Schrader Method 65

3.3 Data Processing 66

3.3.1 Categorical Forecast Verification 66

3.3.2 Verification of the JETRAX Algorithm 68

3.3.3 Verification of the Schumann, Hanson, and Schrader Contrail Forecast Algorithms 69

IV. Data Description and Analysis 71

4.1 Data Description 71

4.1.1 Ground Based Observation Data 71

4.1.2 Aircraft Based Observation Data 74

4.1.2.1 High Bypass Engine Type (C-141) Observations 74

4.1.2.2 Low Bypass Engine Type (F-16) Observations 75

4.2 Data Analysis 76

4.2.1 Measures of Accuracy 76

4.2.1.1 Hit Rate 77

4.2.1.2 Critical Success Index 77

4.2.1.3 False Alarm Rate 78

4.2.2 Measure of Bias 79

4.2.3 Measures of Skill 79

4.2.3.1 Heidke Skill Score 80

4.2.3.2 Kuipers Skill Score 80

4.2.4 Measures of Statistical Significance 81

Page

V. Findings and Conclusions 83

5.1 Results 83

5.1.1 JETRAX Validation 83

5.1.2 Schrader, Schumann, and Hanson Algorithm Validation 85

5.2 Conclusions 88

5.2.1 Conclusions Drawn From JETRAX Validation Study 88

5.2.2 Conclusions Drawn From Algorithm Comparison 89

5.3 Post Analysis 90

5.4 Recommendations for Further Research 94

Appendix A. Saturation Vapor Pressure Calculation Using the Goff-Gratch Equation 96

Appendix B. Radiosonde Comparison 98

Appendix C. Ground Based Contrail Observations 101

Bibliography 116

Vita 119

List of Figures

Figure Page

1. Cross-Sectional View of a High Bypass Turbofan Engine 4

2. An AFWA 30-hour Forecast of Contrail Bases and Tops 7

3. Saturation Vapor Pressure Curve and Exhaust Gases / Ambient Air Mixing Line ..56

4. Saturation Vapor Pressure and Critical Slope 60

5. Determination of Critical Temperatures for Different Values of Relative Humidity. .62

6. 2 x 2 Contingency Table 67

7. Distribution of Temperatures and Flight Levels of Observed Aircraft 72

A1. Plot of Saturation Vapor Pressure vs. Temperature 97

B1. Comparison of Radiosonde Temperature Data 99

B2. Comparison of Radiosonde Dewpoint Data 100

List of Tables

Table Page

1. Corresponding Values of N and ΔT 16

2. Required Increase in Mixing Ratio per Degree Temperature 17
Rise (g $kg^{-1}C^{-1}$) to Maintain Saturation with Respect to Water
in a saturated Atmosphere Undergoing Heating

3. Moisture Available (g $kg^{-1}C^{-1}$) from Exhaust for Maintaining Saturation With 19
Respect to Water in an Atmosphere Undergoing Heating

4. Critical Slope Comparison at 35,000 Feet 33

5. Comparison Between Appleman Contrail Factor and Those Used by Schrader 34

6. Vaisala RS80 Radiosonde Technical Data 50

7. Extract of FAA Flight Log From 29 October 1997 (sector 98) 51

8. Observed Flight Level Conditions 73

9. F-16 Observations of Contrail Formation Onset 75

10. JETRAX Forecast Statistics 84

11. Schumann, Schrader, and Hanson Algorithm Validation Statistics 86

12. Relationship Between Assumed and Observed Flight Level Relative Humidity ... 90

13. Revised Statistical Comparison 92

C1. Observations From 18 September 1997 101

C2. Observations From 19 September 1997 102

C3. Observations From 22 September 1997 102

C4. Observations From 23 September 1997 102

C5. Observations From 24 September 1997 103

C6. Observations From 25 September 1997 103

C7. Observations From 29 September 1997 103

C8. Observations From 1 October 1997 104

C9. Observations From 2 October 1997 105

C10. Observations From 4 October 1997 105

C11. Observations From 5 October 1997 106

C12. Observations From 6 October 1997 106

C13. Observations From 8 October 1997 106

C14. Observations From 9 October 1997 107

C15. Observations From 10 October 1997 107

C16. Observations From 12 October 1997 108

C17. Observations From 13 October 1997 108

C18. Observations From 14 October 1997 109

C19. Observations From 15 October 1997 110

C20. Observations From 16 October 1997 110

C21. Observations From 17 October 1997 111

C22. Observations From 21 October 1997 111

C23. Observations From 22 October 1997 111

C24. Observations From 28 October 1997 112

C25. Observations From 29 October 1997 113

C26. Observations From 30 October 1997 114

C27. Observations From 31 October 1997 115

Abstract

Accurate contrail forecasts allow pilots to avoid levels of the atmosphere which are conducive to contrail formation, reducing their likelihood of being visually detected by enemy forces. The primary objective of this thesis is to evaluate the performance of the JETRAX contrail forecast algorithm currently used by the Air Force Weather Agency to support military air operations.

A total of 397 ground based contrail observations were collected at Wright-Patterson Air Force Base on 27 different days. Observations were collected with the aid of air traffic control radar, which greatly facilitated the positive identification of overflying aircraft and provided necessary information such as aircraft type and flight level. This data set was used to validate corresponding contrail forecasts disseminated to operational users via the Air Force Weather Information Network (AFWIN).

All forecast products derived from the JETRAX algorithm demonstrated greater skill than persistence, climatology, or other algorithms tested with real time radiosonde data. An 84.4 percent accuracy rate was observed. Based on this research, the Air Force Weather Agency is providing excellent contrail forecasts to their operational users, and while there is still room for improvement, no immediate changes to the JETRAX algorithm are warranted.

A VALIDATION STUDY OF THE AIR FORCE WEATHER AGENCY (AFWA) JETRAX CONTRAIL FORECAST ALGORITHM

1. Introduction

1.1 Background

1.1.1 Definition of Contrails

Derived from the words condensation trails, contrails are the long cylindrical clouds which develop behind an airborne aircraft when its wake becomes supersaturated with respect to water (AWS/TR-81/001, 1981:1). Air is supersaturated when its relative humidity exceeds 100 percent, and the condition of supersaturation required for contrail formation may be achieved by two distinct physical mechanisms. One is the rapid pressure drop of air flowing over an airfoil at high speeds, which causes the sudden adiabatic cooling of the trailing vortex to a temperature below that at which the ambient moisture can remain in the vaporous state. The water vapor condenses to water droplets, and aerodynamic contrails are formed. Since aerodynamic contrails are typically short-lived and usually form during sharp evasive maneuvers once the aircraft has already been detected by the enemy, they are not considered an operational forecast problem. Engine exhaust contrails, on the other hand, are considerably more persistent and form at high altitudes, commonly during straight and level flight. Condensation in this case results

when warm, moist exhaust gases saturate their immediate environment upon being thrust into the typically much colder, drier ambient atmosphere. The combustion of a hydrocarbon such as aviation fuel adds heat to the atmosphere, which acts to lower the relative humidity of the wake and makes contrail formation less likely, while simultaneously adding water vapor to the atmosphere, therefore making contrail formation more likely by raising the relative humidity of the wake. When the net effect of these two competing processes is the saturation of the wake, an engine exhaust contrail will form (Coleman, 1996:3). Since this type of contrail is the phenomenon that the JETRAX model was designed to forecast, any further reference to contrails should be understood to mean engine exhaust contrails rather than aerodynamic contrails.

1.1.2 Rationale for Contrail Forecast Verification

Since the very presence of contrails is an irrefutable indication of the actual or recent presence of aircraft, contrails are a form of military intelligence. Although the stealth technology incorporated in the design of our modern aircraft has significantly reduced their effective radar cross section, our modern and conventional aircraft are equally vulnerable to enemy detection with only the human eye when they are producing contrails. Aircrew survivability is thereby jeopardized. Once the enemy has visually detected the aircraft, contrails further aid the enemy in directing defensive countermeasures from the ground and vectoring air intercept forces. Persistent contrails can further hinder the efforts of friendly forces as upper level winds may spread the contrails into large cirrus cloud layers. The resulting reduction to flight level visibility can make the rendezvous of

aircraft and air-to-air refueling more difficult (AWS/TR-81/001,1981:2). Even our tactics can be divulged by persistent contrails as our ingress and egress routes are clearly marked. Accurate contrail forecasts help mission planners and pilots avoid the levels where contrails form. Mission effectiveness is thereby enhanced.

1.1.3 The Air Force Weather Agency JETRAX Contrail Forecast Model

Contrail formation has been of interest to the United States military ever since aircraft capable of flying at the high altitudes required for contrail development entered the inventory. The fundamental approach to forecasting contrails was developed by Herbert Appleman in 1953, and his philosophy is still the foundation upon which numerous contrail forecast algorithms are built today. Appleman asserted that at any given pressure level there is a critical temperature below which contrails are expected to form. The pressure altitude at which the ambient air temperature first becomes colder than this critical temperature is designated as the contrail base, while the pressure altitude at which the ambient air temperature again becomes warmer than the critical temperature is designated as the top of that contrail layer. Prior to 1 June 1995, Air Force Global Weather Central (AFGWC), now the Air Force Weather Agency, produced contrail forecasts based exclusively on Appleman's work.

In response to Air Combat Command's requirement for improved contrail forecasts in 1994, the Air Force weather community conducted a thorough review of the contrail forecasting process. Consequently, the model was updated.

Appleman's original model used only one contrail factor of 0.0336 g $kg^{-1}C^{-1}$. The term contrail factor refers to the ratio of the amount of water vapor generated by fuel combustion to the amount of heat it produced. Separate research efforts conducted by Capt Mark Schrader (Schrader, 1994) and Capt Jeffrey Peters (Peters, 1993) determined that a single contrail factor does not suitably describe this ratio for all types of engines. A second type of ratio, the engine bypass ratio, was taken into consideration for the first time within the framework of contrail forecasting. The bypass ratio is the amount of air which is compressed by the fan stages and bypassed through the fan duct around the core of the engine versus the amount of air that is compressed by the fan stages and passed through the engine core. The engine core consists of the compressor, combustor, and turbine, the components which produce thrust.

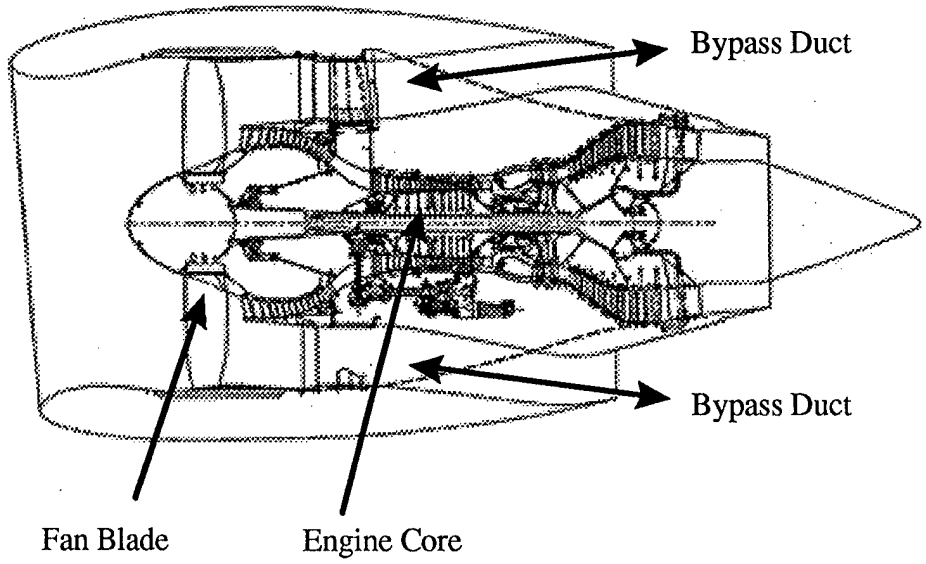

Fig 1. Cross-Sectional View of a High Bypass Turbofan Engine

Some Boeing 777 aircraft use the General Electric GE90 high bypass turbofan engine, which has a 9:1 bypass ratio. This means that nine pounds of air is bypassed around the core for every pound of air sent through the core. By comparison, the Pratt & Whitney F100-PW-229 replacement engine for F-15s and F-16s has a bypass ratio of only 0.36:1, and is considered a low bypass engine. Turbojets are non bypass engines as all the air taken in passes through the core. Turbojets have a bypass ratio of zero, and are typical of the powerplants in use when Appleman conducted his research in the 1950s. Contrail forecasts for high, low, and non bypass engine types have been available for operational use by Air Force weather personnel since 1 June 1995.

At the time of this study, the most recent change to the AFWA JETRAX contrail forecast model has been the 13 January 1997 switch to the Navy Operational Global Atmospheric Prediction System (NOGAPS) global spectral forecast model as the source of its initial data (Laracuente, 1997, personal communication). JETRAX incorporates temperatures, D-values, relative humidities from 700 to 300 millibars, tropopause pressure levels, tropopause heights, and tropopause temperatures as determined by NOGAPS at the 700, 500, 400, 300, 250, 200, 150, 100, 70, 50, and 30 millibar levels. Moisture data above the 300 millibar level is not ingested from the NOGAPS model into JETRAX, but an assumed vertical moisture profile was retained from the earlier Appleman models. Relative humidity is assumed to be 40 percent from the 300 millibar level to 300 meters below the tropopause, 70 percent from 300 meters below the tropopause to 300 meters above the tropopause, and 10 percent at pressure altitudes 300 meters above the tropopause and higher.

Once JETRAX has its initial data, it uses modified Goff-Gratch formulations as described in Appendix A to calculate the critical temperatures required for contrail formation at each NOGAPS grid point. This is done at each millibar level for zero and 100 percent relative humidities and at the tropopause levels where the relative humidity is assumed to be 70 percent. Starting with the lower levels, the algorithm checks to see whether the temperature at each level is colder than the critical temperature for contrail formation. The pressure altitude at which the temperature first falls below the critical temperature is designated as the contrail base. The comparison continues upward in the atmosphere until the ambient temperature again becomes greater than the critical temperature, where the top of the contrail layer is recorded. If the computed layer is less than 2000 feet thick, it is discarded. If there isn't at least 2000 feet between two distinct layers, the layers are combined. At the zulu times of 0000 and 1200 (twice each day), JETRAX computes forecast contrail bases and tops for 18, 24, and 30 hours into the future for high bypass, low bypass, and non bypass engine types. These forecasts are presented on the same 2.5 degree latitude by 2.5 degree longitude grid used by NOGAPS output, and are readily available to military users via the World Wide Web on the Air Force Weather Agency's internet home page. The internet address of this site is http://afwin.offutt.af.mil:443/home.html. An example of the product, the 30-hour forecast for high bypass engine types valid at 1200Z on 25 October 1997, is shown in Figure 2.

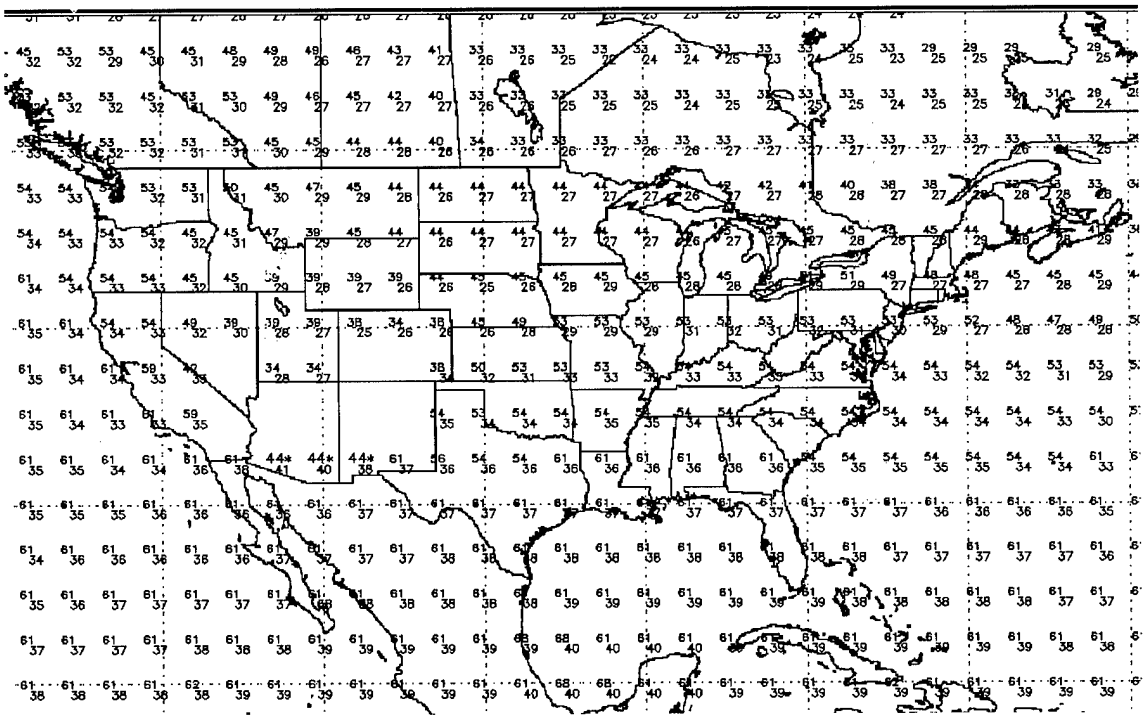

Fig 2. An AFWA 30-hour Forecast of Contrail Bases and Tops

1.2 Problem Statement

1.2.1 Primary Focus of This Research

JETRAX has been ingesting initial data from the Navy's NOGAPS global spectral model since 13 January 1997, but a subsequent validation study to determine the accuracy of the contrail model's output has yet to be performed. How good are the contrail forecasts being produced by the 1997 configuration of the JETRAX model?

1.2.2 Additional Objectives

With motivation ranging from their obvious impact on military operations to their potential impact on the Earth's environment, contrails have been the subject of numerous papers, technical journal articles, and other research efforts. Many of these are summarized in Chapter 2. There were two papers published in 1997 which had a particularly significant influence on the direction and methodology of this research.

The first, An Examination of the Hanson Contrail Forecast Algorithm Under Low Relative Humidity Conditions by Captain Rob Asbury, established a method of directly observing aircraft from the ground in order to build a data set for the purpose of validating contrail forecast algorithms. Included in Asbury's recommendations for further contrail research at Wright Patterson Air Force Base was the suggestion that an earlier observing time would take better advantage of the morning peak in commercial air traffic over the Dayton, Ohio area, thereby yielding a larger, more statistically significant sample size. This was accomplished, and further modification to Asbury's observation method also allowed the data set collected for this research to have a greater balance between "yes" and "no" forecasts. Will the statistical manipulation of this larger, more balanced data set confirm Asbury's finding that the performance of the Hanson algorithm decreases with decreasing relative humidity?

The second paper that provided particular influence on this research was Moisture Sensitivity of Contrail Forecast Algorithms by Capt Allen Rabayda. One of Rabayda's conclusions was that the AFGWC contrail forecast algorithm had an inherent high forecast base bias. This is to say that the forecast bases are too high, and more specifically that

aircraft would commonly begin to produce contrails at lower altitudes than forecast. An effort was made to work with local Air National Guard and Air Force Reserve flying units to determine the base of the contrail level, which was then compared to the AFWA forecast. Do the contrail forecasts generated by the current version of the AFWA JETRAX forecast algorithm also exhibit a high forecast base bias? Rabayda's primary conclusion was that AFGWC could not improve the accuracy of its contrail forecasts by replacing the 40/70/10 assumed relative humidity profile with a more accurate climatological profile. Will comparing the accuracy of other contrail forecast algorithms using near real-time humidity data to that of the current configuration of the JETRAX algorithm support this conclusion?

1.3 The Benefit of Solving the Problem

Once a baseline measurement of the accuracy of the JETRAX model is obtained, it can be determined whether or not further adjustments to the model are warranted. The benefits of an accurate contrail forecast model are obvious when viewed within the context of air operations in a combat scenario. If mission planners are provided an accurate contrail forecast 30 hours in advance, they can select an optimal course and flight level to best avoid contrail formation. If highly accurate 18-hour forecasts are available to military weather personnel, they will be able to brief combat aircrews with information they can use to both reduce the likelihood of their visual detection over hostile territory and enhance their ability to locate enemy aircraft while in flight. Particularly now with the

growing technology gap between the United States military and less sophisticated enemy forces, any opportunity to reduce the chances of visual detection must be fully exploited.

1.4 Approach

1.4.1 Data Collection

On days which provided favorable weather conditions for making ground based observations of overflying aircraft, a radiosonde was launched to obtain a real-time analysis of the atmospheric temperature and moisture profiles. When an aircraft was positively identified, information such as flight level, aircraft type, and whether or not contrails were being produced was recorded. The temperature and relative humidity corresponding to the particular flight level of each aircraft could be readily determined from the radiosonde data. The methodology of associating an observed aircraft to its flight level, as well as to the temperature and relative humidity at that flight level, is described in Chapter 3.

1.4.2 JETRAX Validation

At each grid point, the JETRAX forecast output provides an altitude layer or layers between which contrail formation is expected. For each observed aircraft, the altitude was known, so the next step was to determine whether or not JETRAX forecast contrails for that particular altitude at that particular time. One of four results are possible in such a comparison. The first contingency is where the aircraft is observed to be producing

contrails and JETRAX correctly forecast the occurrence of contrails. Second, the plane could be producing contrails when JETRAX indicated that contrails would not occur at that altitude. The third possibility is that the aircraft is not generating contrails but JETRAX predicted that contrails would occur, while the fourth contingency is a correct forecast of the non-occurrence of contrails. The results of this methodical comparison between observations and forecasts are entered into 2 x 2 contingency tables for ease of statistical manipulation as described in Section 3.3.

1.4.3 Algorithm Comparison

For the purpose of comparison, similar contingency tables were constructed for contrail forecast algorithms developed by Schrader, Schumann, and Hanson. The primary difference is that JETRAX uses forecast parameters from the NOGAPS global spectral model, while the other three algorithms utilized the real-time sounding data to produce their contrail "nowcasts". Although the JETRAX algorithm was at somewhat of a disadvantage to the other three algorithms because its initialization parameters were forecast rather than observed, an indication of its skill against other methods could be inferred.

1.4.4 Exact Bases

Previous contrail forecast validation studies have used a contingency table method similar to the yes/no approach described previously, or have attempted to validate the forecast bases directly with a right/wrong approach. In the latter, "observed" contrail

bases were often taken from pilot reports or simply estimated as being half way between the flight level of the lowest aircraft observed to be producing contrails and that of the highest one not producing contrails. Error is obviously induced using this philosophy, but the degree of precision associated with the forecast bases is nonetheless desirable to quantify. To that end, arrangements were made with local military flying units to attempt to directly determine the exact base of the contrail layer. Though the sample sizes of these *in situ* observations were very much smaller than those of ground based observations, they did provide an exact flight level for the onset of contrail formation for a particular engine type on a particular day. This information is virtually impossible to determine from the ground.

1.5 Thesis Organization

Chapter 2: *Literature Review* presents a chronological discussion of relevant contrail research conducted over the past five decades. Particular attention is given to the 1953 work of Herbert Appleman, the foundation upon which many of today's algorithms are built.

Chapter 3: *Methodology* describes the assumptions made and provides some of the thermodynamic theory upon which contrail forecasting is based. The radiosonde equipment used to measure ambient temperature and relative humidities is described, as are the procedures used in collecting aircraft observations. A summary of the data processing method is also provided.

Chapter 4: *Data Description and Analysis* elaborates on the statistical tools used to determine the validity of the JETRAX forecast model and to compare it to the other algorithms tested.

Finally, Chapter 5: *Findings and Conclusions* presents the results of the data analysis from several different angles, as well as operational recommendations based on this study and suggestions for further research.

2. Literature Review

2.1 *The Formation of Exhaust Condensation Trails by Jet Aircraft*, Herbert Appleman, 1953

Appleman's groundbreaking thermodynamic treatment of the contrail formation process has been referenced by virtually every subsequently written paper pertaining to the subject. In this paper he defined the state of the atmosphere required for contrail formation, elaborated on the physical process itself, and explained the relationship between key factors such as relative humidity, temperature, and pressure.

Clouds may form through a number of different mechanisms, and contrails are in essence mixing clouds. Mixing clouds result when quantities of two distinctly different parcels of air are mixed, and with their union saturation is achieved. The two different types of air parcels that are mixed together to form contrails are engine exhaust and the ambient air through which the plane is flying.

Appleman recognized that the combustion of aviation fuel added both water vapor and heat to the wake of the aircraft, and further stated that the resulting relative humidity of the wake was dependent upon the following factors:

ΔW - moisture added to the environment by the exhaust, which raises relative humidity

ΔH - heat added to the environment by the exhaust, which lowers relative humidity

P - initial pressure of the environment

T - initial temperature of the environment

f - initial relative humidity of the environment

N - the ratio of entrained environmental air to exhaust gas

The ratio described by N varies from zero to infinity, and the rate at which its value increases determines the length of the trail.

Burning one gram of jet fuel was determined to add 12 grams of exhaust gases, 1.4 grams of water vapor, and 10,000 calories of heat to the wake. Each gram of exhaust gases mixes with N grams of the surrounding air. The increase in temperature (ΔT) of the affected environment is:

$$\Delta T = \frac{10{,}000}{12N \times 0.24} \tag{1}$$

Likewise, the amount of water added by the combustion of jet fuel was determined:

$$\Delta W = \frac{1.4 \times 1{,}000}{12N} \tag{2}$$

The ratio of the two is independent of N. With appropriate units and conversion factors,

$$\frac{\Delta W}{\Delta T} = \frac{\dfrac{(1.4\ \text{g}) \cdot \left(\dfrac{1{,}000\ \text{g}}{1\ \text{kg}}\right)}{(12\ \text{g}) \cdot N}}{\dfrac{(10{,}000\ \text{cal}) \cdot \left(4.186 \dfrac{\text{J}}{\text{cal}}\right)}{(12\ \text{g}) \cdot N \cdot \left(1004 \dfrac{\text{J}}{\text{kg} \cdot \text{C}}\right) \cdot \left(\dfrac{1\text{kg}}{1{,}000\ \text{g}}\right)}} \tag{3}$$

This yields the original contrail factor calculated by Appleman:

$$\frac{\Delta W}{\Delta T} = 0.0336 \frac{g}{kg \cdot C} \tag{4}$$

So an aircraft flying through the atmosphere will raise the mixing ratio of the wake 0.0336 g kg^{-1} for each degree of temperature increase. Depending on the initial temperature, pressure, and relative humidity of the atmosphere and upon the value of N, the affected part of the atmosphere may be left either saturated or unsaturated after the passage of the aircraft.

Appleman reasoned that since ΔT depends on N, the amount of temperature increase can be used in place of N in all calculations.

Table 1. Corresponding Values of N and ΔT

delta-T	100	80	60	40	20	10	5	2	1	0.5
N	35	43	58	87	175	350	700	1750	3500	7000

Appleman then created tables showing the increase in mixing ratio per degree of temperature rise required to maintain saturation in initially saturated air which is undergoing heating at different pressure levels, temperatures, and values of ΔT. Wherever the table shows values less than 0.0336 g $kg^{-1}C^{-1}$, the passage of an aircraft would cause an initially saturated atmosphere to become supersaturated with the consequent production of water droplets. The supersaturation of a saturated environment is aided by cold temperatures, high pressures, and increased mixing between the environment and the exhaust (small values of ΔT, large values of N). Where the values are greater than .0336,

the aircraft would leave an initially saturated environment in a subsaturated state, and could even cause evaporation in a cloud in its path, producing a "negative contrail" or "distrail". The asterisk (*) following the values in Table 2 that are less than 0.0336 indicates that the passage of an aircraft would supersaturate the initially saturated atmosphere and result in the formation of contrails at that pressure level.

Table 2. Required Increase in Mixing Ratio per Degree Temperature Rise ($g\ kg^{-1}C^{-1}$) to Maintain Saturation With Respect to Water in a Saturated Atmosphere Undergoing Heating

		Temperature (C)				
	delta T (C)	-40	-50	-60	-70	-80
1000 mb	5	0.0154*	0.0059*	0.0020*	0.0006*	0.0002*
	40	0.0926	0.0436	0.0192*	0.0078*	0.0029*
500 mb	5	0.0308*	0.0117*	0.0040*	0.0013*	0.0004*
	40	0.1864	0.0875	0.0384	0.0156*	0.0058*
100 mb	5	0.1544	0.0587	0.0201*	0.0062*	0.0017*
	40	0.9822	0.4466	0.1935	0.0778	0.0291*

Appleman constructed a similar table for the saturation of an initially unsaturated atmosphere undergoing heating. If contrails are to form in an environment that is not initially saturated, some of the water from the aircraft exhaust must be used to saturate the air with respect to water at its initial temperature, and the remainder to maintain saturation during the temperature rise caused by the heat from the exhaust. Appleman defined the following variables involved in this process, all with respect to water:

w - initial mixing ratio of the environment (grams of water vapor to kilograms of dry air)

w_{sw} - saturation mixing ratio (mixing ratio required for saturation)

f_w - relative humidity (ratio of the current mixing ratio to the saturation mixing ratio at the same temperature and pressure, ((w) / (w_{sw}(p,T)))

δw - the amount of water which must be furnished by the exhaust to raise the relative humidity of the affected environment to 100 percent at the initial temperature and pressure.

Δw - the amount of water available to maintain saturation of the environment as it is heated by the exhaust.

Defined mathematically,

$$w = w_{sw}\left(\frac{f_w}{100}\right) \tag{5}$$

$$\delta w = w_{sw}\left(1 - \frac{f_w}{100}\right) \tag{6}$$

and

$$\Delta w = \frac{1.4 \times 1{,}000}{12N} - w_{sw}\left(1 - \frac{f_w}{100}\right) \tag{7}$$

The ratio of Δw and ΔT now becomes:

$$\frac{\Delta w}{\Delta T} = 0.0336 - \left(\frac{1}{\Delta T}\right) w_{sw}\left(1 - \frac{f_w}{100}\right) \tag{8}$$

which describes the moisture, in g kg^{-1} per Celsius degree temperature rise, available for maintaining saturation during the passage of the aircraft.

Table 3. Moisture Available (g $kg^{-1}C^{-1}$) from Exhaust for Maintaining Saturation With Respect to Water in an Atmosphere Undergoing Heating

			Temperature (C)				
	delta T (C)	fw (%)	-40	-50	-60	-70	-80
1000 mb	5	100	0.0336	0.0336	0.0336	0.0336	0.0336
		0	0.0102	0.0257	0.0312	0.0330	0.0335
	40	100	0.0336	0.0336	0.0336	0.0336	0.0336
		0	0.0307	0.0326	0.0333	0.0335	0.0336
500 mb	5	100	0.0336	0.0336	0.0336	0.0336	0.0336
		0	0	0.0178	0.0288	0.0324	0.0333
	40	100	0.0336	0.0336	0.0336	0.0336	0.0336
		0	0.0278	0.0316	0.0330	0.0334	0.0336
100 mb	5	100	0.0336	0.0336	0.0336	0.0336	0.0336
		0	0	0	0.0098	0.0273	0.0321
	40	100	0.0336	0.0336	0.0336	0.0336	0.0336
		0	0.0044	0.0237	0.0306	0.0328	0.0334

In the case of an initially subsaturated environment, the amount of moisture available to maintain saturation (per degree of temperature increase) decreases with low pressure and relative humidity, high temperature, and with increased mixing between the exhaust and the environment. From the values calculated in Table 3, curves were constructed showing the amount of moisture available from the exhaust (g $kg^{-1}C^{-1}$) after the relative humidity of the environment has been raised to 100 percent at its initial temperature. From Table 2, curves were drawn showing the amount of moisture necessary to maintain saturation in

saturation in saturated air undergoing heating. The intersections of the two sets of curves determine, for a given value of pressure and mixing, the critical initial temperature of the environment which must exist for the formation of a trail saturated with respect to water. A warmer temperature would leave the trail subsaturated, as the environment would require more moisture than was available from the fuel, and contrails would not form. A colder temperature would lead to supersaturation and contrail formation.

Appleman further surmised that it is not only necessary for the water vapor from the fuel combustion to raise the relative humidity of the entrained environment to 100 percent with respect to water, but also some visible water must be produced. As soon as the water begins to transform from liquid to solid, the contrail, which had been at approximately 100 percent relative humidity with respect to water, becomes highly supersaturated with respect to ice. The excess water vapor immediately begins to sublime onto the ice particles, resulting in the production of larger and larger crystals until a final relative humidity of approximately 100 percent with respect to ice is reached in the trail. Whereas the initial relative humidity of the environment is given with respect to water, the final relative humidity of the trail is given with respect to ice. Following the previously used notation, the excess moisture available after the environment is brought to saturation with respect to ice, Δw, can be written:

$$\Delta w = w_{si} - w = w_{si} - w_{sw}\left(\frac{f_w}{100}\right) \qquad (9)$$

where w_{si} is the saturation mixing ratio with respect to ice.

It follows that

$$\Delta w = \frac{1.4 \times 1{,}000}{12N} - \left(w_{si} - w_{sw} \frac{f_w}{100} \right) \tag{10}$$

and

$$\frac{\Delta w}{\Delta T} = 0.0336 - \frac{1}{\Delta T} \left(w_{si} - w_{sw} \frac{f_w}{100} \right) \tag{11}$$

The excess moisture available after the entrained environment has been brought to ice saturation at its initial temperature is always greater than if the trail had been brought to water saturation. In addition to the moisture required to maintain saturation with respect to ice during the temperature rise caused by the exhaust, sufficient moisture must also be present to satisfy the visible water content requirement of at least 0.004 g m^{-3} for a faint trail and 0.010 g m^{-3} for a distinct trail. The intersections of the curves of required and available moisture define the values of critical temperature for the existence of a trail saturated with respect to ice and with a visible water content of the specified amount. Depending on the initial temperature, pressure, and relative humidity of the environment and upon the ratio of the entrained environment to the exhaust, the temperature required to form a trail saturated with respect to water may be colder or warmer than the temperature required to form a trail saturated with respect to ice but with a visible water content of 0.004 or 0.010 g m^{-3}. Since both requirements must be satisfied, the colder of the two temperatures in each case is the critical temperature which must exist for the formation of a visible contrail. Therefore, in order to determine the critical temperature, composite graphs showing both sets of curves must be used. Since the entire formation

region is colder for the formation of water trails than for the corresponding ice trails in all cases, the critical temperature for the formation of water trails also satisfies the requirement for both faint and distinct ice trails.

Appleman mentioned that the relative humidity measurements as obtained from radiosonde observations at low temperatures were both inaccurate and few in number. In the complete absence of data, the assumption that the relative humidity was in the vicinity of 40 to 90 percent in the upper troposphere and between zero and 60 percent in the stratosphere was shown to induce an error in critical temperature of only three or four degrees. These estimates could be further refined by noting the source of the upper flow and the presence or absence of cirrus clouds. He concluded with a summary of his three main assumptions, which to this day still provide the foundation of contrail prediction theory:

1. The wake behind the aircraft must somewhere reach saturation with respect to water before any of the water vapor in the exhaust gases can be transformed into visible water.
2. After the water droplets have formed, immediate freezing will occur and the excess water vapor in the trail will deposit onto the ice crystals until the relative humidity in the trail is reduced to 100 percent with respect to ice.
3. An ice crystal content of 0.004 g m^{-3} is required for a faint trail and 0.010 g m^{-3} for a distinct trail.

It was found that the third assumption had no effect on the formation of the trail, but did affect its dissipation. Appleman felt that as experience was gained with specific types of

aircraft, fairly accurate forecasts would become practicable not only as to whether contrails would occur, but also as to their density and persistence.

2.2 *A Further Analysis of Contrail Data*, Air Weather Service, 1953

Air Weather Service Technical Report 105-112 (AWS TR 105-112) presented the results of an analysis of contrail observations received at Headquarters, Air Weather Service through 28 March 1953. The report basically tested the validity of Appleman's contrail forecasting technique and also offered guidance to field units conducting their own contrail studies. The majority of the observations were of Air Force B-47, B-36, and B-29 multiengine aircraft over the continental United States and Alaska, and "MiG Alley" reports from F-86 single engine jet fighter aircraft during the Korean War.

Contrail formation was still a relatively new phenomena at the writing of this report, and the data that had been collected led its authors to the following, admittedly contradictory, conclusions:

1. Contrails never occur in the stratosphere
2. Contrails never occur above a certain number of thousand feet above the tropopause
3. Once contrails begin to form, no top will be reached
4. Contrails always occur above a certain pressure level

The report stated that the tropopause is a factor in contrail formation only with respect to the temperature and relative humidity values existing at its level. Thus when the tropopause level is moist and/or cold enough, statements "3" and "4" are true, and when the tropopause is dry and/or warm enough, statements "1" and "2" are true. All four

statements were believed to be true under certain circumstances based on the available data, but none was believed to be true as a general statement. The importance of ambient relative humidity and the unavailability of accurate humidity measurements was also highlighted. AWS TR 105-112 was rescinded in 1957.

2.3 *Derivation of Jet Aircraft Contrail Formation Curves*, Herbert Appleman, 1957

Air Weather Service Technical Report 105-145 (AWSTR 105-145) presented new tables and graphs and reviewed Appleman's original procedures with regard to contrail formation and forecasting. The most significant new data considered by this report came from Project Cloud Trail, an airborne data collection effort within the Air Defense Command in conjunction with Air Weather Service. Between 1 December 1954 and 15 December 1955, jet aircraft from 36 fighter-interceptor squadrons based in the United States accumulated data to serve as the basis for improved methods of forecasting contrails, cirrus clouds, haze, and turbulence. Pilots recorded many parameters, including the occurrence and nonoccurrence of contrails, and forwarded their findings to Headquarters, Air Weather Service for processing. Citing the difficulty of obtaining accurate measurements of relative humidity at the levels where contrails typically form, contrail probability curves were constructed as a function of only temperature and pressure. Forecasters in the field could use the plots of contrail frequency versus temperature and contrail probability versus temperature and pressure to provide yes/no forecasts to pilots and mission planners.

The paper further broke the data down into geographical and seasonal effects on contrail probability. Appleman again stated that an assumed relative humidity profile could be used in lieu of in-situ measurements at high altitudes.

2.4 *Prediction of Aircraft Condensation Trails*, PROJECT CONTRAILS, James E. Jiusto, 1961

The Office of Naval Research authorized the Cornell Aeronautical Laboratory to conduct a study of the basic characteristics of aircraft exhaust contrails for the purposes of evaluating existing methods for predicting their occurrence, developing refined criteria upon which contrail forecasting can be improved, and generating information to assist in the eventual suppression of contrails.

While Jiusto did not discount the methods or relevance of Appleman's work, the results of his research did lead him to the three following findings:

1. The contrail factor ($\Delta W / \Delta T$), the ratio that expresses the change in moisture content and temperature in the aircraft exhaust wake, is better represented by a value of 0.0295 g $kg^{-1}C^{-1}$ rather than the 0.0336 g $kg^{-1}C^{-1}$ put forth by Appleman. Critical temperatures for contrail formation are thereby shifted by approximately one degree Celsius to colder values.
2. The criterion for a visible contrail, namely one possessing a water concentration of 0.004 g m^{-3}, is valid only for idealized conditions of observation. Optimum viewing conditions involve a forward scattering angle of the sun's rays and a contrasting sky background. Under less favorable viewing conditions, a contrail may require upwards of 0.1 g m^{-3} of condensate in order to be visible.

3. There is strong evidence that the final phase of contrails is not always ice. Contrails that remain in the liquid phase will require colder temperatures (two to three degrees colder) to satisfy the minimum visibility criterion of 0.004 g m^{-3}, and will always be non-persistent.

Jiusto asserted that contrail duration is a function of ambient relative humidity, final condensate phase, contrail density, and atmospheric diffusion characteristics. He stated that contrails consisting of ice particles, the more common situation, will persist for hours if the environmental conditions exceed ice saturation, i.e., exceed ambient relative humidity values of approximately 60 to 70 percent. When ambient relative humidity is less than ice saturation, contrails comprised of ice crystals will sublime in seconds to minutes, depending on contrail density.

Certain recognizable weather patterns were determined to be of use in the forecasting of contrails where accurate knowledge of temperature and humidity at the pressure level of interest is not complete. Jiusto offered the following meteorological conditions and geographic climatology to augment standard prediction techniques and provide a guide for the planning of long range military operations:

A. Good Flight Paths - Generally Unfavorable for Contrail Formation

1. High pressure areas in the upper troposphere and low pressure areas in the lower stratosphere (below 25 km).

2. Latitudes north of 50 degrees north latitude in the stratosphere (200-100 mb) during the summer, and mid-latitudes between 40 and 60 degrees north latitude at 100 mb during the winter season.

3. South of 35 degrees north latitude in winter and south of 60 degrees north latitude in summer at 300 mb (upper troposphere).

4. On the left side of jet streams looking downstream, 100-300 miles from the jet axis. For "warm" jet streams, the jet core itself may be included.

5. 10,000 feet or more above the tropopause, temperature criteria for the appropriate level permitting. A dry environment should be assumed.

6. Areas of negative vorticity advection at 300 mb or where cirrus clouds are absent, temperature criteria permitting.

B. Flight Paths to Avoid - Generally Favorable for Contrail Formation

1. Low pressure areas in the upper troposphere and high pressure areas in the lower stratosphere.

2. The entire 200 mb level in winter. At 100 mb, south of 45 degrees north latitude in summer; south of 40 degrees north latitude and north of 60 degrees north latitude in winter.

3. North of 35 degrees north latitude in winter and north of 60 degrees north latitude in summer at 300 mb.

4. On the right side of jet streams looking downstream, up to about 400 miles from the axis.

5. The tropopause level plus or minus about 2000 feet.

6. Areas of positive vorticity advection at 300 mb or where cirrus clouds are present.

In addition to re-drawing contrail formation curves based on a $\Delta W / \Delta T$ value of 0.0295 g $kg^{-1}C^{-1}$ rather than the 0.0336 g $kg^{-1}C^{-1}$ calculated by Appleman, Jiusto provided

an alternate graphical means of determining contrail formation that truly provided insight into the cloud physics of contrails. He used a phase diagram with the plot of the saturation mixing ratio curve relative to water versus temperature at a given pressure level and compared the air-exhaust mixture to the curve. Straight lines having the slope $\Delta W / \Delta T = 0.0295$ g $kg^{-1}C^{-1}$ were drawn to indicate the changing conditions of moisture and temperature in the exhaust wake as mixing with the environment progresses. If the temperature and relative humidity place the mixture to the left of the line drawn tangent to the curve, the air-exhaust mixture exceeds water saturation and a contrail will be formed. An indication of the density of the contrail is given by the degree to which water saturation is exceeded.

2.5 *Contrails Forecasting*, James E. Jiusto and Roland J. Pilie, 1964

This manual provided a more thorough presentation of the material covered in Jiusto's 1961 paper, and was also prepared for the Office of Naval Research by the Cornell Aeronautical Laboratory of Cornell University. The belief that contrails could consist of liquid water instead of ice and the contrail factor of 0.0295 g $kg^{-1}C^{-1}$ were maintained from the previous paper, the same graphical approaches were restated, and a greater emphasis was placed upon the analysis of synoptic and climatological data for the purpose of producing long range estimates of contrail occurrence.

2.6 *Forecasting Aircraft Condensation Trails*, Air Weather Service, 1981

Though generally a republication of the earlier Air Weather Service contrail forecasting manuals, this technical report (AWS/TR-81/001) adds a brief description of the computer program used at Air Force Global Weather Central to forecast the bases and tops of layers of the atmosphere within which contrails are expected to occur. Because of operational considerations, a maximum of two contrail layers are retained for each grid point. The program assumes relative humidity values of 40 percent from 500 mb to approximately 300 meters below the tropopause, 70 percent within 300 meters above and below the tropopause, and 10 percent in the stratosphere. The use of an assumed humidity profile and the retention of no more than two contrail layers for any given grid point as described in this paper are still true of the JETRAX algorithm currently in use.

2.7 *SAC Contrail Forecasting Algorithm Validation Study*, Walter F. Miller, 1990

This project report by the United States Air Force Environmental Technical Applications Center documented the evaluation of a new RC-135 contrail forecast algorithm called SACFCST along with three versions of an Air Weather Service computer algorithm that differed only by the value they assumed for relative humidity. TROPFCST determined the relative humidity by using the 40/70/10 assumption given in AWS/TR-81/001. DRYFCST assumed relative humidity to be zero while WETFCST assumed it to be 100 percent. A collection of 484 pilot reports from SAC RC-135 aircraft between 1984 and 1987 provided the basis of the evaluation, but only 90 of the 484 observations in the original database did not involve contrails. Because the data was

skewed to such a degree, a pessimistic algorithm was favored and contrails were overforecast. It was determined that SACFCST was not an improvement over the TROPFCST algorithm in use at the time. Additionally, when WETFCST and DRYFCST were compared, relative humidity was seen to be the determining factor for forecasting contrails in 45 percent of the cases.

2.8 *New Techniques for Contrail Forecasting*, Jeffrey L. Peters, 1993

Advancements in aircraft power plants, particularly the development of bypass turbofan engines, prompted a new contrail forecast study by Air Weather Service. AWS/TR-93/001 described the development of new contrail forecast algorithms for several types of engines used in modern aircraft, and also provided contrail forecasting rules that correlate synoptic scale upward vertical motion with contrail formation.

Previous data analyses had indicated that contrail formation was being underforecast below 40,000 feet but overforecast above 40,000 feet. As a result, the study was conducted in two parts. For the study of contrail formation at and below 40,000 feet, contrail observations were collected from SAC KC-135, RC-135, EC-135, B1-B, and B-52 aircraft from 1 May 1990 to 30 April 1991. Aircrews reported date and time of the observation, pressure altitude, corrected outside air temperature, latitude, longitude, and contrail condition. The database consisted of 4,387 such observations, 1,121 of which were of contrail occurrences and 3,266 were of non occurrences. Correlations between contrail formation and both temperature and vertical motion were drawn. A similar statistical analysis was performed on a high altitude data set, a collection of 1,040 contrail

observations taken above 40,000 feet by U-2 and TR-1 aircraft from May 1990 to August 1991.

For data at or below 40,000 feet, both the Appleman method and Air Force Global Weather Central (AFGWC) 18-hour forecast correctly predicted the nonoccurrence of contrails in 98 percent of the cases. Their verification statistics for correctly predicting the occurrence of contrails, however, were much worse. The Appleman method correctly predicted the occurrence of contrails in 27 percent of the cases, while the AFGWC 18-hour forecast only predicted the occurrence of contrails 24 percent of the time. Both methods had comparable false alarm rates. The ratio of incorrect forecasts to the number of times the event was forecast was about 20 percent for the Appleman and AFGWC methods for both the occurrence and nonoccurrence of contrails observed at 40,000 feet and below.

The forecast verification statistics for the data taken above 40,000 feet were strikingly different than those for 40,000 feet and below. The Appleman method yielded correct forecasts for the occurrence of contrails above 40,000 feet 95 percent of the time with a false alarm rate of 27 percent, while the AFGWC 18-hour forecast correctly predicted contrail occurrence 64 percent of the time with a 16 percent false alarm rate. The trends were reversed for contrail nonoccurrence above 40,000 feet. The statistics for the Appleman method dropped to 46 percent for correctly predicting nonoccurrence and a 12 percent false alarm rate, while the AFGWC verification statistics went up to 80 percent correct and a 43 percent false alarm rate. Both methods showed considerably better skill above 40,000 feet than at 40,000 feet and below.

Since both methods were correctly predicting contrail formation in the troposphere only about one fourth of the time, many SAC aircraft were producing contrails when they theoretically should not have been. This fact, and particularly the tremendous drop seen in the Appleman method's accuracy of forecasting contrail nonoccurrence when evaluating high flying U-2 aircraft data, led to the development of engine-specific contrail forecast algorithms.

Different types of engines add different proportions of moisture and heat to the ambient atmosphere, and the single critical slope of 0.0336 g $kg^{-1}C^{-1}$ used by Appleman is inadequate for the jet engine types in use today. Engine characteristic data for non bypass turbojet, low bypass turbofan, and high bypass turbofan powerplants was obtained from the Pratt & Whitney Aircraft Engine division of United Technologies. Engine exhaust characteristics, specifically tailpipe moisture and temperature, were determined for a wide range of power settings, Mach numbers, and flight levels. New critical slopes were then calculated for various flight levels.

Table 4. Critical Slope Comparison at 35,000 feet

Method	Engine Type	Critical Slope
Appleman	Constant	0.0336 g/kgC
Peters	Non Bypass	0.0360 g/kgC
	Low Bypass	0.0400 g/kgC
	High Bypass	0.0490 g/kgC

Use of the different critical slopes results in significantly different critical temperatures for contrail formation. The critical slopes were not only different for each engine type, but they also found to vary slightly with flight level as well. In each case, the new engine specific forecast algorithms showed better forecast skill than the Appleman method.

2.9 *Calculations of Critical Temperature of Contrail Formation for Different Engine Types*, Mark L. Schrader, 1994

Schrader developed the basis for the JETRAX contrail forecast algorithm currently used by the Air Force Weather Agency. This paper by Schrader updates that by Peters with newly obtained contrail factors and the correction of two errors Peters made in his derivation of the Appleman diagrams. First, where Peters calculated critical temperatures for contrail formation using the saturation vapor pressure with respect to an ice surface, Schrader claims that the saturation vapor pressure with respect to a water surface should be used. This is because it is generally accepted that the water vapor from the exhaust condenses to liquid droplets before freezing. Since the vapor pressure over water is higher than that over ice, the wake becomes supersaturated with respect to ice upon freezing. Schrader also corrects Peters' use of a linear interpolation for determining the critical temperature lines for 10, 40, and 70 percent relative humidity. While linear interpolation can be used from the critical temperature at 100 percent relative humidity to the critical temperature at zero percent relative humidity (since $e/e_s=1$ at the tangent point of the e-T curve and $e/e_s=0$ at zero percent relative humidity), the critical temperature lines for the intermediate relative humidities are not equally spaced. Schrader stated that one must map the linear function in e-T space to a non linear function in RH-T space.

This update to the original Appleman contrail forecasting nomograms using the corrected method of Peters and an explicit derivative of the Goff-Gratch formula for vapor pressure over a water surface was incorporated into the new JETRAX contrail forecast model, which became operational at Air Force Global Weather Central in May 1995. The contrail factors employed by Schrader are as follows:

Table 5. Comparison Between Appleman Contrail Factor and Those Used by Schrader

Method	Engine Type	Critical Slope
Appleman	Constant	0.0336 g/kgC
Schrader	Non Bypass	0.0300 g/kgC
	Low Bypass	0.0340 g/kgC
	High Bypass	0.0390 g/kgC

2.10. *A Reexamination of the Formation of Exhaust Condensation Trails by Jet Aircraft*, Harvey M. Hanson and Douglas M. Hanson, 1995

Hanson and Hanson attempted to refine the basic Appleman method and develop an algorithm which would provide a theoretical prediction of contrail formation that demonstrated better agreement with the available empirical data, particularly in a high altitude, low relative humidity environment. They state that while previous techniques yield results that are consistent with the empirical data for saturated conditions where relative humidity is equal to 100 percent, there is an increasing discrepancy as the computations are taken toward lower relative humidity values.

Hanson and Hanson emphasize the fact that the vapor pressure versus temperature curve is not linear. In fact, it approaches the zero value of vapor pressure in an

asymptotic manner. They state that in order to correctly account for decreasing relative humidity, the approach should be to find the equivalent temperature point that would provide a saturation condition that contains the same mass of water per unit volume as is present under the reduced relative humidity observed at the higher temperature. The critical temperature for contrail formation under subsaturated conditions is calculated by first considering the mass of water vapor per unit volume involved in the mixing process. The point on the saturation vapor pressure curve where this amount of water vapor would result in saturation is then determined. The lowest temperature where this condition is satisfied is the critical temperature for contrail formation at the reduced relative humidity. Although critical temperatures can not be determined when using this method if the relative humidity is zero percent, Hanson and Hanson claim that such critical temperatures would be so low as not to be characteristic of the portion of the atmosphere under consideration.

The Hansons' algorithm uses the same contrail factors Schrader used, as shown above in Table 5. They conclude their paper by claiming that their algorithm provides a significantly improved accuracy in the theoretical prediction of the probability of contrail formation, particularly at lower relative humidity values, and that more accurate humidity measurements would allow more accurate contrail prediction.

2.11 *Pilot Alert System Flight Test Final Report*, P. Saatzer, 1995

A flight test program was conducted by the Northrop Corporation from January 1992 to March 1993 in order to evaluate the performance of two competing prototype sensor

systems for the real-time, in-flight detection of contrail occurrence. Such a Pilot Alert System would provide an indication in the cockpit that contrails were being produced, prompting the pilot to change altitude in order to make enemy detection less likely. One system developed by the General Electric Corporation was based on camera image processing technology, while the second system developed by OPHIR Corporation was based on a laser radar or lidar technique. The sensors were installed on a T-33 aircraft, which would gradually climb to an altitude suitable for the formation of contrails. A Northrop Lear 35 aircraft instrumented with the Astrovision system was used as a chase plane, providing both video documentation for the flight test and verification of contrail onset occurrences to determine the reliability of the two sensors. The T-33 would continue to climb until observers detected the onset of contrail formation. After the contrail was well established, the T-33 would then descend to an altitude at which contrail formation was not possible. This process was repeated as many times as atmospheric conditions and fuel constraints allowed for each flight. After logging about 100 flight hours, it was determined that the General Electric system provided correct detections on only 37 percent of the 50,000 data points, while the OPHIR system was found to provide correct responses on 76 percent of 46,000 data points.

In the process of validating the performance of the two Pilot Alert System prototypes, a data base of about 800 contrail observations was acquired. These observations cover contrail onset altitudes from 28,000 to 38,000 feet, onset temperatures from -46 to -56 degrees Celsius, and relative humidities from 10 to 90 percent. Different seasons and different synoptic situations were also encountered.

2.12 *Validation of the Appleman Contrail Forecasting Scheme Using Engine Specific Aircraft Data*, David J. Speltz, 1995

In an effort to validate a new Appleman-based contrail forecasting scheme using different contrail factors, Speltz looked at a new set of contrail observations. He used the same relative humidity assumptions of 40 percent in the troposphere, 70 percent within 300 meters of the tropopause, and 10 percent in the stratosphere used by the current Air Force Weather Agency JETRAX contrail forecast algorithm.

His results indicated that the contrail factors of 0.030 g $kg^{-1}C^{-1}$ for non bypass, 0.034 g $kg^{-1}C^{-1}$ for low bypass, and 0.039 g $kg^{-1}C^{-1}$ for high bypass engine types used by Schrader performed more poorly than the higher values of 0.036, 0.040, and 0.049 g $kg^{-1}C^{-1}$ determined by Peters. He found that the most accurate forecasts were for stratospheric contrails and noted that the forecasts of tropospheric critical temperatures were frequently 10 Celsius degrees colder than the temperatures at which contrail formation was observed. He felt that assuming a constant relative humidity in the comparatively dry stratosphere was an acceptable practice because small changes in low relative humidity values have a considerably less significant effect on critical temperature than do small changes in high relative humidity values. Speltz contended that the accuracy of contrail forecast algorithms would improve when improvements in forecasting relative humidity were achieved.

2.13 *On Conditions for Contrail Formation From Aircraft Exhausts*, Ulrich Schumann, 1996

Schumann begins with the classic Appleman mixing cloud theory but he takes into consideration the fact that some of the heat of combustion is converted into kinetic energy and dissipated in the aircraft's trailing vortex system. Since heat lowers relative humidity and decreases the likelihood of contrails, the removal of this heat from the initial contrail formation process by mechanical means has the net effect of increasing the likelihood of contrails. This is the explanation given for contrails that are observed to form at warmer ambient temperatures than predicted by the Appleman method alone.

To quantify the effect of this heat dissipation, Schumann defined propulsion efficiency η as the amount of work performed against the aircraft drag compared to the combustion heat. Propulsion efficiency is defined in terms of:

F - thrust

V - true air speed

Q - specific combustion heat

M_F - rate of fuel flow

$$\eta = \frac{F \cdot V}{Q \cdot M_F} \tag{12}$$

A typical value of η for modern high bypass turbofan engines is between 0.3 and 0.4, which is higher than that of older non bypass turbojets or low bypass turbofans. Schumann noted that the propulsion efficiency accounts for the same changes that were

covered with engine specific parameters by Peters (1993), but η accounts not only for the engine performance but also for the aircraft speed and aerodynamic drag.

Schumann estimates critical temperatures for subsaturated conditions with relative humidity values between zero and 100 percent by performing a Taylor series expansion about the point where the engine mixing line is tangent to the saturation vapor pressure curve. This point is where the critical temperature for contrail formation occurs for the case of 100 percent relative humidity. The critical temperatures obtained using this method are in good agreement with those obtained by Schrader. Schumann further looked at the effect of alternative fuels on contrail formation, and determined that if a typical modern wide body airliner burned liquid hydrogen or liquid methane fuels instead of kerosene fuel, the contrails would appear at 10 Celsius degrees warmer ambient temperatures for liquid hydrogen and 4.5 Celsius degrees warmer ambient temperatures for liquid methane. The contrails formed using these fuels would also be geometrically thicker and longer than those produced using conventional jet fuel.

2.14 *Comments on "A Reexamination of the Formation of Exhaust Condensation Trails by Jet Aircraft"*, Ulrich Schumann, 1996

Schumann states that the Hansons' method is equivalent to the classical Appleman approach when the atmosphere is saturated, but no physical reasoning is given for their departure from classical theory as the atmosphere becomes drier. The critical temperature for contrail formation predicted by the Hansons' algorithm approaches minus infinity as relative humidity goes to zero, while classical theory always produces a finite value for critical temperature even for perfectly dry air. Ambient conditions must be somewhere

on the mixing line which tangents the saturation vapor pressure versus temperature curve. Schumann further states that results from the Hansons' algorithm deviate even more strongly from observed contrail conditions than does classical theory. The Hanson and Hanson theory computes extremely low critical temperatures for very dry ambient conditions such as those which prevail in the stratosphere, where short contrails are commonly observed despite low relative humidities of typically less than ten percent. In contrast, Hanson and Hanson suggest that the humidity must be above 25 percent in order to explain 95 percent of previously observed contrails.

2.15 *A New Formulation for the Critical Temperature for Contrail Formation,* Rich F. Coleman, 1996

Coleman derived an analytical expression to compute the critical temperature for contrail formation in terms of water vapor mixing ratio and pressure rather than relative humidity and pressure. He states that this approach avoids the potential forecast errors associated with the temperature sensitivity inherent in relative humidity. Coleman claims that his formulation demonstrates a clear superiority to the critical temperature forecasts of earlier methods because of its reduced sensitivity to errors or uncertainties in the input atmospheric variables.

2.16 *SUbsonic aircraft: Contrail and Clouds Effects Special Study (SUCCESS),* NASA, 1996

SUCCESS is a National Aeronautics and Space Administration (NASA) field program using scientifically instrumented aircraft and ground based measurements to investigate

the effects of subsonic aircraft in terms of contrails, cirrus clouds, and atmospheric chemistry. The program has several objectives. One is to better determine the radiative properties of cirrus clouds and of contrails so that satellite observations can be used to better determine their impact on the earth's radiation budget. SUCCESS hopes to determine how cirrus clouds form and whether or not the exhaust from subsonic aircraft presently affects the formation of cirrus clouds. If it is shown that the exhaust does affect cloud formation, the next step would be to determine whether the changes induced are of climatological significance. Other objectives include paving the way for future studies by developing and testing several new instruments, and better determining the characteristics of gaseous and particulate exhaust products from subsonic aircraft and their evolution in the region near the aircraft.

The most recent SUCCESS field campaign was conducted from Salina, Kansas, from April 8 to May 10, 1996. A medium altitude DC-8 aircraft was used as an *in situ* sampling platform, while a T-39 carrying a suite of instruments designed to measure particles and gases was used to sample the exhaust from the DC-8. The third aircraft used was a high flying ER-2, which acted as a satellite and allowed remote sensing observations to be related to the *in situ* parameters measured by the DC-8 and T-39.

Analysis of the data acquired during this airborne contrail research effort was still under way at the writing of this thesis, but preliminary inspection of the Polarization Diversity Lidar (PDL) data set reveals that a large number of contrails were captured at unmatched spatial resolutions. The 1.06 μm backscattering data were collected in a manner that preserved the 1.5 meter spatial and 0.1 second time resolutions of the PDL

device. Contrails viewed at this scale contain a wealth of information regarding their fine structures, which will help illuminate fundamental properties related to their radiative impact.

2.17 *A Diagnostic Study of the Global Coverage by Contrails*, Robert Sausen, Klaus Gierens, and Ulrich Schumann, 1997

This study estimated the global distribution of contrail formation potential and contrail cloud coverage using meteorological analysis data for temperature and humidity from the European Center for Medium-range Weather Forecasting (ECMWF) and an aircraft fuel consumption data base. Regions with humidity between ice and liquid saturation and with temperature low enough to allow the onset of contrail formation are identified as regions in which persistent contrails may be formed. The frequency with which a region is conditioned for such persistent contrail formation measures the contrail formation potential. Maximum contrail potential was found in the area of the Inter-tropical Convergence Zone near the equator, where most airline flight levels are still below the tropopause and the maximum of upper tropospheric humidity is found. Present day contrail coverage was calculated by multiplying the potential contrail coverage by fuel use. The maximum contrail coverage was found to be about five percent over the eastern United States, as compared to the annual and global mean value of 0.11 percent.

There are concerns that the predicted annual growth of air traffic will result in a continued increase in global contrail coverage. Among the many variables examined by this study was the impact of flight altitude on contrail formation. At the present time, about 40 percent of the air traffic in the North Atlantic flight corridor is above the

tropopause. Shifting this traffic to higher altitudes would move more aircraft into the dry stratosphere, diminishing contrail cloudiness at mid latitudes. The opposite would be recommended for short range airline traffic within the United States or Europe. Shifting this traffic to lower altitudes would move it into warmer ambient air, making contrail formation less likely.

2.18 *Surface Based Observations of Contrail Occurrence Frequency Over the U.S., April 1993-April 1994*, Patrick Minnis, J. Kirk Ayers, and Steven P. Weaver, 1997

Participating in a joint project between the Air Force and NASA, weather observers stationed at 19 different military installations in the continental United States recorded the daytime occurrence of contrails and cloud fraction on an hourly basis from April 1993 to April 1994. Each observation consisted of one of four main categories to describe the current contrail condition: unobserved, non-persistent, persistent, and indeterminate. Additional classification includes whether or not cirrus was also observed in each report. Contrail occurrence was found to vary substantially with location and season with a mean annual frequency of occurrence in unobstructed viewing conditions of 13 percent. A significant correlation was shown to exist between mean contrail frequency and aircraft fuel usage above 7 kilometers, suggesting predictive potential for assessing future contrail effects on climate.

2.19 *Contrail Cirrus and their Potential for Regional Climate Change*, Kenneth Sassen, 1997

Professor Kenneth Sassen of the University of Utah Department of Meteorology reviewed the indirect evidence for the regional climatic impact of contrail generated cirrus clouds and presented a variety of new measurements indicating the nature and scope of the problem. His assessment concentrated on polarization lidar and radiometric observations of persisting contrails from Salt Lake City, Utah, an area which earlier studies had identified as being affected by relatively heavy air traffic. Sassen considered contrail properties such as hourly and monthly frequency of occurrence, height, temperature, relative humidity, visible and infrared radiative impacts, and microphysical content evaluated from *in situ* data and contrail optical phenomena such as halos and coronas. Sassen concludes that the direct radiative effects of contrails do indeed display the potential for causing regional climate change at many midlatitude locations, but that the unusually small particles typical of many persisting contrails may favor the albedo cooling rather than the greenhouse warming effect.

2.20 *An Examination of the Hanson Contrail Forecast Algorithm Under Low Relative Humidity Conditions*, Robert P. Asbury III, 1997

Asbury tested the contrail forecast method of Schumann and of Hanson and Hanson, and compared the results to those obtained using the Schrader technique which was in operational use at Air Force Global Weather Central. The primary focus of Asbury's research was to validate the Hansons' claim that their algorithm provided better contrail forecasts under comparatively dry atmospheric conditions. Using contrail observations

that he personally collected at Wright-Patterson Air Force Base and the data set collected by the Northrop Corporation while evaluating the Pilot Alert System prototypes, Asbury validated each algorithm for a variety of varied parameters. Though all methods detected roughly 75 percent of observed contrail occurrences under moist atmospheric conditions, the performance of the Hanson and Hanson algorithm ironically dropped sharply with decreasing flight level relative humidity, exactly the opposite effect of what its authors had claimed. For this reason, the Hansons' algorithm was not recommended for operational use.

2.21 *Moisture Sensitivity of Contrail Forecast Algorithms*, Allen C. Rabayda, 1997

Rabayda looked at using more representative climatologically based relative humidity profiles in contrail forecast algorithms as opposed to the assumed profile of 40 percent in the troposphere, 70 percent near the tropopause, and 10 percent in the stratosphere used by AFGWC. Intuitively one might assume that the input of more accurate relative humidity data into a contrail forecast algorithm would yield significantly more accurate contrail forecasts, but Rabayda found that this was not the case. Relative humidity variations of more than 30 percent were shown to change the forecast contrail base by less than 1,000 feet. It was demonstrated that, in general, the degree to which forecast bases are affected by relative humidity greatly depends on the atmospheric lapse rate. These results led the author to recommend that AFGWC not replace their 40/70/10 percent assumed relative humidity profile with new satellite derived relative humidity climatologies. Rabayda also concluded that AFGWC's contrail forecast algorithm has an

inherent high forecast base bias, which means that contrails are commonly seen to occur at lower flight levels than the algorithm had forecast.

3. Methodology

3.1 Data Collection

3.1.1 Ground Based Contrail Observations

Observations of overflying aircraft were taken at Wright-Patterson Air Force Base, Ohio between 18 September and 31 October 1997. On days when weather permitted ground-based contrail observations to be made, a radiosonde was launched so that a real-time profile of atmospheric pressure, temperature, and relative humidity could be obtained. Information such as the time of passage and whether or not a contrail was being produced was recorded for each aircraft observed. Once the aircraft were positively identified and the flight level at which they were flying was determined, the radiosonde data was used to assign the appropriate ambient temperature and relative humidity to each particular aircraft. This combination of visual yes/no contrail observations and radiosonde data was entered into three different contrail forecast algorithms so that the accuracy of their individual critical temperature formulations could be determined. The accuracy of the JETRAX-based forecasts from the Air Force Weather Agency was verified on a simple yes/no basis, so only a visual observation and the flight level of each aircraft were needed.

3.1.1.1 Radiosonde Launches

Prior to recording contrail observations, a radiosonde was launched. Each "weather balloon" release was coordinated in advance with the Dayton Flight Service Office of the Federal Aviation Administration (FAA) so that a Notice to Airmen (NOTAM) could be disseminated for the purpose of alerting pilots to the balloon's location. Final launch clearances were requested from the Wright-Patterson air traffic control tower to ensure that the balloon would not interfere with any air traffic in the local area.

The National Weather Service office in Wilmington, Ohio is less than 30 miles away from Wright Patterson, and they launch a radiosonde and provide upper air data every twelve hours. Their data was not used in this research, however, because it may not have corresponded with the optimal time for taking local contrail observations, nor would the vertical resolution of the data have been sufficient for matching accurate values of temperature and relative humidity to each aircraft's flight level. The launch of a research quality radiosonde just before beginning to take observations ensured that the high resolution temperature and humidity information received was as representative of the current state of the atmosphere as possible. A comparison of the Wilmington sounding to data received from two research quality radiosondes is shown in Appendix B.

Once an aircraft operating in controlled airspace reaches the altitude of 18,000 feet, the pilot will set the altimeter to 29.92 inches of mercury, which is the assumed standard sea level barometric pressure in what is referred to as "the Standard Atmosphere". From this level, referred to as Flight Level 180, and above, pilots fly at assigned flight levels that correspond to fixed pressure values. By standardizing the altimeter setting and flying

along fixed pressure levels, all aircraft have the same frame of reference in terms of altitude. The potentially disastrous possibility of two pilots thinking that they are at different altitudes when they are in fact on a collision course is thereby eliminated.

The fact that the national aviation system in this country assumes the same standard atmosphere that meteorologists do greatly facilitates the comparison of aircraft data to meteorological data received from the radiosonde. Since aircraft flight levels relate directly to fixed pressure values, one simply finds the pressure value on the radiosonde data that corresponds to the particular flight level of interest and reads the values of the meteorological variables that were measured at that pressure level. For example, if an aircraft at FL 350 was observed and one wanted to know what the temperature and relative humidity was at its flight level, the pressure value of 238 millibars would be located on the radiosonde data and the corresponding temperature and relative humidity would be recorded. Since FL 350 is always at a pressure of 238 millibars, whatever meteorological variables are measured at 238 millibars can be taken to represent the state of the atmosphere through which the aircraft was flying. This direct relationship between atmospheric pressure and aircraft flight levels served as the basis for determining the flight level temperature and relative humidity of every aircraft that was observed.

During the course of this research, all radiosonde launches used the same equipment: a 100 gram balloon and compressed helium; a Vaisala RS80 model radiosonde consisting of a capacitive BAROCAP® pressure sensor, a THERMOCAP® temperature sensor, a HUMICAP® capacitance thin film humidity sensor; and a Vaisala ground receiving system. More information on the Vaisala UR 15 Ultra High Frequency (UHF)

Radiosonde Receiver and PP 15 Sounding Processor used in this research can be obtained by contacting their manufacturer at PL 26, SF-00421 Helsinki, Finland. Parameters such as height, ascent rate, pressure, temperature, dewpoint, and relative humidity were measured approximately every 1.5 seconds, generating sounding data with tremendous vertical resolution. This humidity sensor in particular has the reputation of providing excellent long-term stability, plus a reliable response at low temperatures and after passing through clouds. Since contrail formation depends heavily on the pressure, temperature, and relative humidity at flight level, it is critically important to measure these parameters as accurately as possible. The range, resolution, and accuracy of the RS80 sensors are shown in Table 6.

Table 6. Vaisala RS80 Radiosonde Technical Data

	Pressure	Temperature	Relative Humidity
Measuring Range:	1060 to 3 millibars	+60 to -90 C	0 to 100 percent
Resolution:	0.1 mb	0.1 C	1 percent
Accuracy:	0.5 mb	0.2 C	less than 3 percent

3.1.1.2 Observation of Aircraft

Once the tower granted permission to launch the balloon, aircraft observations were begun. While the radiosonde data was being received by the Vaisala system at the 88th Weather Squadron, aircraft were spotted overhead using essentially the same method employed by Capt Rob Asbury in his 1996-1997 research efforts. A video camera with a telescopic lens provided 120X magnification along with the ability to record the aircraft

on tape. Subsequent review of the tape greatly aided positive identification of the planes as aircraft type and even the airline could often be easily discerned. Each aircraft could be interrogated frame-by-frame if necessary. When these observations were compared to the FAA flight logs for the corresponding time periods, the majority of the aircraft could be positively matched to their flight levels as indicated in the log. An extract from the FAA log is shown in Table 7.

Table 7. Extract of FAA Flight Log From 29 October 1997 (Sector 98)

AC IDENT	ENTRY TIME	EXIT TIME	ENTRY MEANS	EXIT MEANS	AC CAT	AC TYPE	FP TYPE	FLIGHT PLAN	FLIGHT LEVEL
SWG 417	1402	1404	FM-S88	TO-S83	A/C	DC9	OVER	DTW to FLL	FL 330
LN83LJ	1404	1410	FM-S97	TO-S88	MIL	LR23	ARRV	EWR to IND	FL 410
COA81	1415	1429	FM-S97	TO-S99	A/C	B757	OVER	EWR to SFO	FL 310
UPS2901	1420	1430	FM-S99	TO-S97	A/C	B747	OVER	ONT to PHL	FL 370
AAL33	1421	1431	FM-S97	TO-S99	A/C	B767	OVER	JFK to LAX	FL 350
TWA372	1421	1440	FM-S89	TO-ZCC	A/C	DC9	OVER	STL to EWR	FL 330

The balloon would eventually reach such high altitudes, typically in excess of 60,000 feet, that either the radiosonde's UHF signal would become unreadable or the balloon itself would have expanded beyond its capacity and ruptured due to the low external atmospheric pressure. Both events result in the termination of data receipt. At this time, the data was saved to a text file and the observing site was transferred to the Wright-Patterson air traffic control tower.

Though the area outside the 88th Weather Squadron and a nearby observation tower were both viable locations for the collection of contrail observations, it was noted that it

was always easier to notice an aircraft that was producing a contrail than one which was not. Aircraft flying at high altitudes but not producing contrails are difficult to spot initially, and they are even harder to hold in view and identify with the telescope. Small private or corporate jets in particular are often assigned to flight levels above FL 400 (more than 40,000 feet) and are very difficult to notice with the unaided eye unless they're producing contrails. Because "conning" aircraft were more readily observed than planes which weren't "conning", the data base of observations would inevitably be skewed with a disproportionately large number of aircraft which were producing contrails. The statistical significance of any conclusions drawn from such a data base could therefore be questioned.

In an attempt to alleviate this problem, arrangements were made with Wright-Patterson air traffic control (ATC) personnel to use their Digital Bright Radar Indicator Tower Equipment (DBRITE) scope to aid in aircraft identification while taking observations from their control tower. The DBRITE in the Wright-Patterson ATC tower was basically a remote display of the Dayton International Airport's approach radar. The airspace over the Wright-Patterson area is under FAA positive control and aircraft operating in controlled airspace are equipped with Mode C altitude encoding transponders, which continuously transmit an aircraft's call sign, type, airspeed, and flight level (Slattery, 1998). Transponders substantially increase the ability of a radar to see an aircraft (AIM, 1990) and better enable air traffic controllers to monitor and maintain required separation between all aircraft under their control. The tower's Flight Data System terminal and DBRITE scope made obtaining the desired information from

overflying aircraft a relatively easy process. When a high altitude aircraft was observed to be passing near the Wright-Patterson tower on the DBRITE scope, it was then only a matter of going onto the catwalk outside the tower cab and using the telescope to visually confirm the aircraft type and record whether or not a contrail was being produced. By modifying the observation process to include the use of the DBRITE, virtually 100 percent of observed aircraft could be positively identified. Another benefit was the fact that one would no longer expect more observations to be contributed to the data base on a day favorable for contrail formation than a day where contrail formation was not likely. A data set with a greater balance between "yes" and "no" contrail observations could now be expected.

3.1.2 Airborne Contrail Observations

The ground-based observation method described above is sufficient for building a data base against which the yes/no accuracy of AFWA contrail forecasts can be validated, which is the main objective of this research. The same data base can further be used to validate a number of other contrail forecast models in a similar manner. The data collected from the ground could not, however, be used to determine the exact altitude of the base of the contrail layer on a given day. This level could only be estimated as being somewhere between the altitude of lowest aircraft observed to be producing a contrail and that of the highest aircraft not producing a contrail. Even such a rough approximation as this could not be made if none of the aircraft observed were conning, or vice versa. The AFWA forecasts provide the level of both bases above which and the tops beneath which

contrails are expected to form, so aircraft flying at a flight level between the bases and tops are expected to produce contrails while aircraft outside the contrail layer are not. Though bases are forecast by the JETRAX-generated products from the AFWA, it is difficult to determine how close the forecast bases actually are to the level at which the onset of contrail formation would actually occur.

The much appreciated cooperation of nearby Ohio National Guard and Air Force Reserve flying units was obtained in a limited effort to determine the exact base of the contrail level for low bypass and high bypass engine types. Since the high altitudes necessary to induce contrail formation are not frequently achieved during routine training missions, there were only a few opportunities for airborne contrail observations to be made.

The 445th Airlift Wing (445 AW) of the Air Force Reserve is stationed at Wright-Patterson, and they fly C-141 Starlifter military transport aircraft which are each powered by four high bypass turbofan engines. One 445 AW aircraft was modified by scientists of the Air Force Research Laboratory at Wright-Patterson to test an airborne lidar apparatus. Referred to as the Interim Operational Capability Lidar (lidar is an acronym for *Light Detection and Ranging*), the system uses a laser to measure the speed and direction of winds between the aircraft and the ground in order to improve C-141 high-altitude airdrop accuracy. When the testing took the aircraft to high altitudes, the opportunity was seized to look out the cockpit and rear cargo compartment windows and watch for the onset of contrail formation. This observed contrail base would then be compared to representative radiosonde data and the forecast base for that period of time.

A similar effort was made to determine the base of the contrail level for low bypass engines, specifically those powering F-16 fighter aircraft flown by the Ohio Air National Guard based in Springfield, Ohio. Pilots who were scheduled to fly air-to-air training missions were asked to check and see at what level the onset of contrail formation took place and report the observed contrail base after returning from the sortie. Just as with the high bypass observations from the C-141, these low bypass observations were matched with sounding data and the accuracy of the contrail forecasts were examined.

3.2 Theory

3.2.1 Mixing Cloud Theory

Assuming no losses or additions of heat to the system, the contrail formation process may be assumed to be adiabatic (no change in heat) and isobaric (constant pressure), and can therefore be represented on a hygrometric (vapor pressure versus temperature) chart. The two different entities that are to be mixed, which in this case are the engine exhaust gases and the ambient air, can each be represented as points on the chart. Let the exhaust gases with mass M_1, temperature T_1, and specific humidity q_1, be represented by Point 1 on the chart in Figure 3. Specific humidity is defined as the mass of water vapor per unit mass of moist air (Rogers and Yau, 1996:17). Similarly, let the ambient air through which the aircraft is flying be represented by Point 2 and have mass M_2, temperature T_2, and specific humidity q_2.

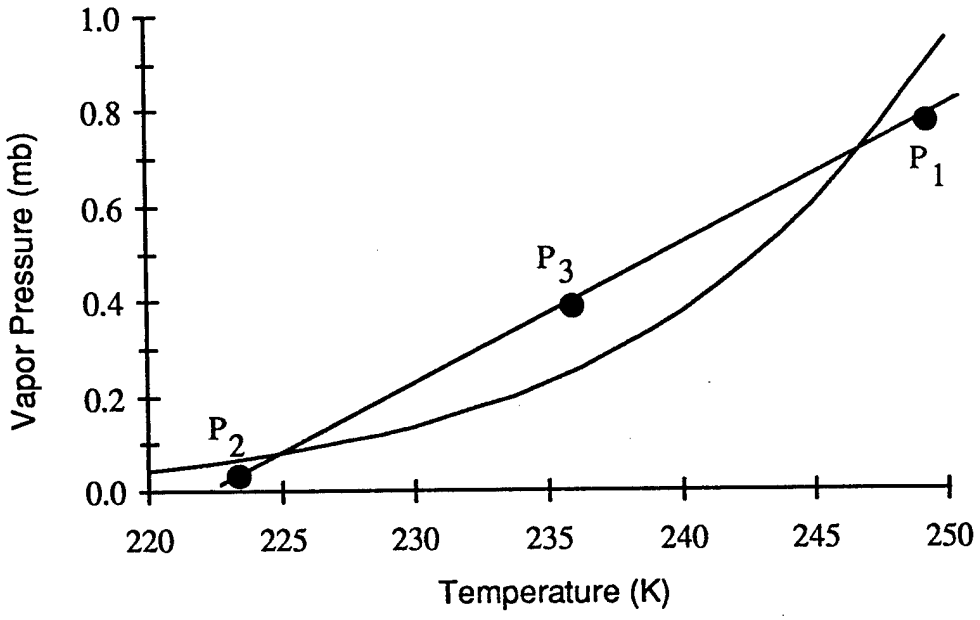

Fig 3. Saturation Vapor Pressure Curve and Exhaust Gases / Ambient Air Mixing Line

Next, assume that the samples represented by Point 1 and Point 2 are thoroughly mixed together at the same pressure. The resulting mixture in the wake of the passing aircraft is represented by Point 3 in Figure 3. The specific humidity of the wake is taken to be the mass weighted average of q_1 and q_2, the specific humidities of the exhaust gases and ambient air, respectively.

$$q_3 \approx \frac{M_1}{M_1 + M_2} \cdot q_1 + \frac{M_2}{M_1 + M_2} \cdot q_2 \tag{13}$$

Specific humidity (q) is related to vapor pressure (e) through pressure (p) and the ratio (ε)

of the mass of water vapor to the mass of dry air, such that $q \approx \varepsilon e p^{-1}$ (Rogers and Yau, 1996:17). The value of ε is taken to be 0.622 and both e and p have the units of millibars. Just as the specific humidity of the mixture is the mass weighted average of the two individual specific humidities, it follows that the vapor pressure of the mixture is the mass weighted average of the two vapor pressures, e_1 and e_2:

$$e_3 \approx \frac{M_1}{M_1 + M_2} \cdot e_1 + \frac{M_2}{M_1 + M_2} \cdot e_2 \tag{14}$$

Since contrail formation is assumed to be an adiabatic process, no net gain or loss of heat will occur in the system during mixing. Therefore, the amount of heat gained by the ambient air is exactly equal to that lost by the exhaust gases:

$$M_1(c_p + w_1 c_{pv})(T_1 - T_3) = M_2(c_p + w_2 c_{pv})(T_3 - T_2) \tag{15}$$

where

c_p = specific heat of dry air at constant pressure (J deg^{-1} kg^{-1})

c_{pv} = specific heat of water vapor at constant pressure (J deg^{-1} kg^{-1})

w_1 = mixing ratio of the exhaust gases (g kg^{-1})

w_2 = mixing ratio of the ambient air (g kg^{-1})

T_3 = equilibrium temperature of the mixture (deg)

Since the mixing ratios are negligible as compared to the other terms, the previous equation reduces to the mass weighted average of the temperatures of the exhaust gases and ambient air:

$$T_3 \approx \frac{M_1}{M_1 + M_2} \cdot T_1 + \frac{M_2}{M_1 + M_2} \cdot T_2 \tag{16}$$

As previously indicated by Figure 3, the temperature and vapor pressure of the wake (Point 3) corresponds to some position on the straight line connecting Points 1 and 2 on the hygrometric chart. The temperature and vapor pressure of the mixture, (T_3,e_3), depends on the ratio of M_1 to M_2. If the mass of the exhaust gases in the mixture is greater than the mass of ambient air, then Point 3 will lie closer to M_1 with respect to the midpoint of the line, reflecting the warmer temperature and higher water vapor content of the exhaust gases.

The Clausius-Clapeyron equation expresses the change of saturation vapor pressure with temperature (Rogers and Yau, 1996:14). The saturation vapor pressure curve, as drawn in Figure 3, is simply the locus of points on the hygrometric chart where the relative humidity equals 100 percent (Wallace and Hobbs, 1977:93-95). The Clausius-Clapeyron equation can be written:

$$\frac{de_s}{dT} = \frac{L}{T\left(\alpha_2 - \alpha_1\right)} \tag{17}$$

where

$\frac{de_s}{dT}$ = derivative of saturation vapor pressure with respect to temperature

L = latent heat of vaporization (J kg^{-1})

α_1 = specific volume of the liquid state at temperature T (m^3 kg^{-1})

α_2 = specific volume of the vapor state at temperature T (m^3 kg^{-1})

If an ordered pair of temperature and vapor pressure lies above and to the left of the saturation vapor pressure curve, as does Point 3 in Figure 3, a supersaturated condition exists at that point. Any point lying directly on the saturation vapor pressure curve represents a saturated condition, while subsaturated conditions are found at all points to the right of and below the curve. Relating the hygrometric chart again to contrail formation, contrails would form at Point 3, but conditions are too warm at Point 1 and too dry at Point 2 for 100 percent relative humidity to be exceeded. The conditions for saturation are however met when the two unsaturated air parcels are mixed together. This is how mixing clouds are formed.

3.2.2 Forecasting Contrail Formation

As explained in Chapter 2, the contrail factor is the ratio of water to heat added to the atmosphere by engine exhaust. The JETRAX algorithm uses three different engine-specific contrail factors to generate contrail forecasts for high, low, and non bypass engine types. The contrail factor may be used to determine the critical slope, which is the slope of the line on the hygrometric chart which is both tangent to the saturation vapor

pressure curve and passes through the point representing the temperature and vapor pressure of the exhaust gases. The critical slope is given by (Schrader, 1994:7):

$$\frac{\Delta e}{\Delta T} \approx \frac{p}{622} \frac{\Delta \omega}{\Delta T} \tag{18}$$

The critical slope is illustrated in Figure 4 below:

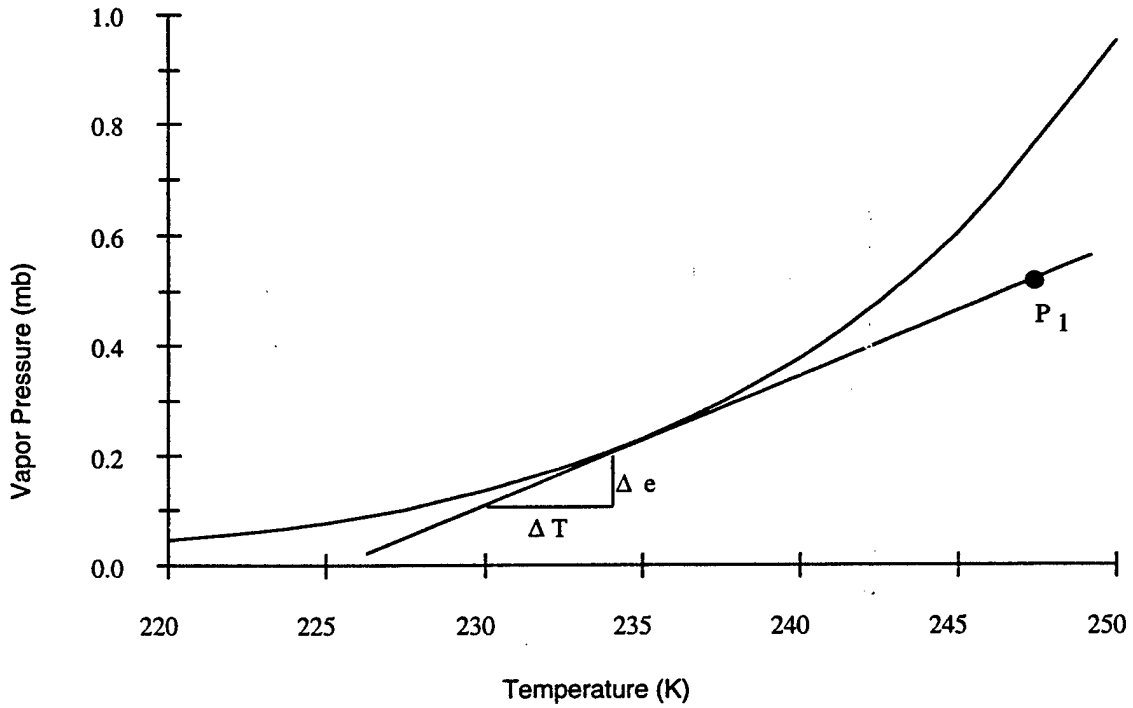

Fig 4. Saturation Vapor Pressure and Critical Slope

The line tangent to the curve through Point 1 with slope $\Delta e/\Delta T$ represents a set of critical temperatures as a function of ambient relative humidities. For environmental conditions

lying to the left of this line on a hygrometric chart, mixing of the exhaust gases (still represented by Point 1) with the ambient air will result in the supersaturation of the wake and therefore contrail formation. The slope of such a line would be less than that of the critical slope, and the temperature of the ambient air would be colder than the critical temperature at a given pressure. Environmental conditions to the right of the critical line, on the other hand, would not result in contrail formation. The mixing line would not cross the saturation vapor pressure curve at any point, and the temperature if the ambient air would be warmer than the critical temperature required for contrail formation.

The critical line tangent to the saturation vapor pressure curve on a hygrometric chart may be used to determine the critical temperature required for contrail formation when the environment is saturated with respect to water. The relative humidity equals 100 percent under these conditions, and the critical temperature (T_C) is determined by the temperature value at the point of tangency.

When the ambient relative humidity is less than 100 percent, some of the water vapor from the exhaust gases is used to bring the wake to saturation before contrails may begin to form. The critical temperature for subsaturated conditions is determined by finding the temperature at the point where the critical line for that particular value of initial relative humidity first crosses the saturation vapor pressure curve on the left. As with any initial value of relative humidity, contrails will form anywhere the ambient temperature is colder than T_C. Though the critical line in Figure 4 represented only the critical temperatures for saturated conditions, critical lines of the same critical slope can be drawn for any value of relative humidity. For decreasing relative humidities, the lines are farther to the left,

which makes physical sense because colder critical temperatures would be required in order for relative humidity to reach 100 percent. Critical lines for 100 percent and 10 percent relative humidity at a constant pressure of 500 millibars are plotted with the saturation vapor pressure curve on the hygrometric chart in Figure 5.

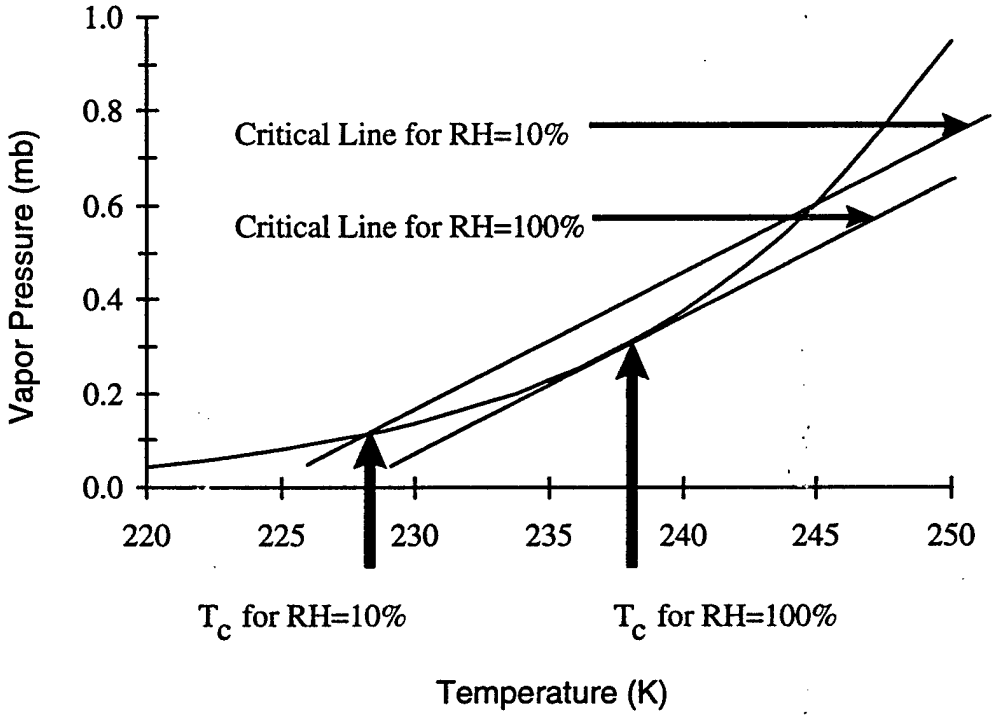

Fig 5. Determination of Critical Temperatures for Different Values of Relative Humidity

3.2.3 Critical Temperature Formulations

For the purpose of comparison, the values of ambient pressure, temperature, and relative humidity measured during the radiosonde launches were entered into three different contrail forecast algorithms. Though all three are based on Appleman's method of determining a critical temperature, each algorithm has a slightly different approach that

resulted in different critical temperatures for the same pressure and relative humidity values.

3.2.3.1 Schumann Method

Schumann calculates the critical slope of the mixing line ($\Delta e/\Delta T$) as a function of the propulsion efficiency of the aircraft. Different types of engines will have different propulsion efficiencies just as other contrail forecast methods use different contrail factors in their calculations.

$$G = \frac{EI_{H2O} c_p p}{\varepsilon Q(1 - \eta)} \tag{19}$$

where

G = critical slope

EI_{H2O} = the emission index of water vapor for the fuel burned (kg kg^{-1})

c_p = the specific heat of air at constant pressure (J deg^{-1} kg^{-1})

p = the pressure at flight level (mb)

ε = 0.622 (unitless)

Q = the specific combustion heat of the fuel burned

η = propulsion efficiency (unitless)

After calculating the critical slope, the next step is to determine the temperature at which the mixing line is tangent to the saturation vapor pressure curve. This will be the critical temperature for 100 percent relative humidity. The value of the critical temperature is

calculated by setting the derivative with respect to temperature of the saturation vapor pressure equation equal to the critical slope and solving for the temperature at the point of tangency. The temperature where both slopes are equal is the critical temperature for contrail formation when the relative humidity is 100 percent (Schumann, 1996:10). Critical temperatures for zero percent relative humidity may be obtained explicitly, but the critical temperatures for intermediate values of relative humidity are found by performing a Taylor series expansion about the T_C value for 100 percent relative humidity Schumann, 1996:10,18).

3.2.3.2 Hanson Method

Hanson and Hanson calculated the critical slope of the mixing line by converting the contrail factor (g kg^{-1} C^{-1}) to units of vapor pressure per degree (mb C^{-1}) as shown below:

$$\frac{\Delta e}{\Delta T} = \frac{p\,(C_F)}{622} \tag{20}$$

Similar to the Schumann method, the critical temperature for saturated conditions is determined by equating the critical slope to the saturation vapor pressure slope and implementing an iterative process to find the temperature that satisfies the equation. In a marked departure from classical theory, the Hansons then found critical temperatures by multiplying the critical slope of the saturation vapor pressure curve by the correction factor 100/RH and solving for temperature. A critical temperature can therefore not be determined for perfectly dry (zero percent relative humidity) ambient conditions because the division by zero would result in an undefined value (Hanson and Hanson, 1995:2402-2403).

3.2.3.3 Schrader Method

The Hanson and Schrader models both use a similar method for calculating critical temperatures for saturated conditions, but for conditions less than 100 percent relative humidity, their approaches differ significantly. First, Schrader finds the vapor pressure at the critical temperature for a given relative humidity by linear interpolation:

$$e\left(T_{C,RH}\right) = e_s\left(T_{C,100}\right) - \left(T_{C,100} - T_{C,RH}\right)\frac{de_s}{dT}\Big|T_{C,100} \qquad (21)$$

where

$e(T_{C,RH})$ = vapor pressure at a given relative humidity (mb)

$e_s(T_{C,100})$ = saturation vapor pressure at the critical temperature for 100 percent relative humidity (mb)

$T_{C,100}$ = critical temperature at 100 percent relative humidity (K)

$T_{C,RH}$ = critical temperature at a given relative humidity (K)

$\frac{des}{dT}|T_{C,100}$ = derivative of the saturation vapor pressure curve with respect to temperature, evaluated at the critical temperature for saturated conditions (mb K^{-1})

Using the Goff-Gratch formula for saturation vapor pressure and the definition of relative humidity in terms of vapor pressure and saturation vapor pressure, a relationship in terms of relative humidity and critical temperature can be found (Schrader, 1994:8-9):

$$\frac{e(T_{C,RH})}{e_s(T_{C,RH})} \times 100 = RH \qquad (22)$$

where

$e_s(T_{C,RH})$ = saturation vapor pressure at given value of relative humidity (mb)

RH = relative humidity (%)

This equation is then solved by an iterative process such that the critical temperature makes both sides of the equation equal (Schrader, 1994:9).

3.3 Data Processing

3.3.1 Categorical Forecast Verification

Categorical forecasts are those that consist of a statement, with no expression of uncertainty, that one and only one set of finite possible outcomes will occur. The predictands under these circumstances are discrete, meaning the observed variable can take on only one set of possible values. In this study, the forecast is simply a "yes/no" expression that contrails will or will not occur, and contrails are either observed ("yes") or not observed ("no"). Such forecast problems are easily analyzed using a 2 x 2 contingency table (Wilks, 1995:238).

The 2 x 2 contingency table is a display of absolute frequencies, or counts, of the four possible combinations of event forecast and event observed pairs. A model of the contingency table used in this study is shown in Figure 6.

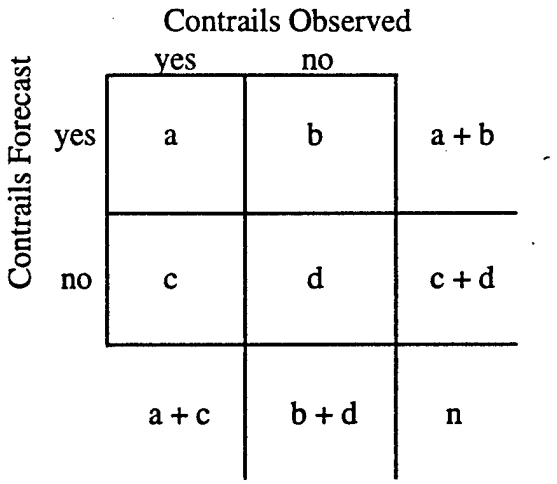

Fig 6. 2 x 2 Contingency Table (Wilks, 1995:239)

There are four possible combinations of forecast/observation pairs:

1. Contrails are forecast and observed to occur (entry a).
2. Contrails are forecast but are not observed to occur (entry b).
3. Contrails are not forecast but are observed to occur (entry c).
4. Contrails are not forecast and are not observed to occur (entry d).

The process of building the contingency tables is not complete until every day's forecast from each algorithm under study has been verified against each of that day's aircraft observations. Other information available from the table is the total number of times contrails were forecast (a + b), the total number of times that contrails were not forecast

to occur (c + d), the total number of contrails observed (a + c), the total number of "non-conning" observations (b + d), and the sample size, or total number of aircraft observed (a + b + c + d = n). A perfectly accurate forecast would produce a contingency table with zero entries for "b" and "c" along the lower left to upper right diagonal. Under these circumstances, all "yes" forecasts would be accompanied by observed contrails, and all "no" forecasts would correctly predict no observed contrails (Wilks, 1995:240). For imperfect forecasts with nonzero entries for "b" and/or "c", statistical measures of accuracy and skill are employed to distinguish between competing forecast methods. These methods will be described in Chapter 4.

3.3.2 Verification of the JETRAX Algorithm

Forecasts from each model run were retrieved from the AFWA home page on the World Wide Web, and the predicted bases and tops were recorded in a data log. A total of nine forecasts were produced for the continental United States with each model run, specifically a 30, 24, and 18 four forecast for each of the three engine types, high bypass turbofans, low bypass turbofans, and non bypass turbojets. At least one entry was made into the contingency table for each aircraft observed. For example, a contrail observation taken at the Greenwich Mean Time of 1200Z could be compared to the 18-hour forecast from the current model run as well as a 30-hour forecast from the previous day's model run since both forecasts have the same 1200Z valid time for the same day. Separate contingency tables were constructed for 18-hour forecasts, 24-hour forecasts, 30-hour forecasts, high bypass aircraft, low bypass aircraft, "low RH" days, "high RH" days, and

finally for all observations. The determination of whether a day had high relative humidity or low relative humidity could only be made on days when reliable radiosonde data was acquired, but each of the other contingency tables could be populated with all visual contrail observations that were made of positively identified aircraft. For example, if the JETRAX algorithm had forecast the contrail level to be from Flight Level 350 (FL 350) to FL 600 for high bypass engines and an aircraft with a high bypass engine was observed to be producing a contrail at FL 350, then an "a" entry was made into the appropriate contingency tables. The event was forecast to occur and the event was observed to occur. If, however, that high bypass aircraft had been producing contrails at FL 330, a "c" entry would be made because the event was not forecast to occur but it was observed to occur. In this case, a contrail was forming below the flight level at which the model had predicted they should occur.

3.3.3 Verification of the Schumann, Hanson, and Schrader Contrail Forecast Algorithms

Though a similar method was used to measure the accuracy of all the algorithms being studied, the Schumann, Hanson, and Schrader algorithms could not be verified unless upper air sounding data corresponding to each aircraft observation was available. Values of flight level temperature and relative humidity were essential for the critical temperature formulations of each algorithm to be both calculated and verified. The Schrader and Hanson algorithms additionally required a value of contrail factor while the Schumann algorithm uses propulsion efficiency.

Each observed aircraft was matched to the conditions of the ambient air at its flight level. If the flight level temperature is colder than the critical temperature calculated by one of the algorithms, then in effect a "yes" forecast had been made by the algorithm. If that aircraft was observed to be producing a contrail, then that forecast was correct and an "a" entry was made into the appropriate contingency tables. Had the ambient temperature been warmer than the critical temperature, it would have been taken to be a "no" forecast by the algorithm. The incorrect forecast for the aircraft that had been observed producing a contrail would be represented by a "c" entry in the contingency tables.

Chapter 4 will discuss what information can be inferred from contingency table data.

4. Data Description and Analysis

4.1 Data Description

4.1.1 Ground Based Observation Data

Approximately 470 aircraft were observed during the data collection phase of this research, of which 397 were positively identified. The flight levels of the positively identified aircraft ranged from FL 310 (31,000 feet in the Standard Atmosphere, or 287 millibars) to FL 450 (45,000 feet in the Standard Atmosphere, or 147.4 millibars). Radiosonde data was available to assign a flight level temperature and relative humidity to 333 of these 397 aircraft. Based on the World Meteorological Organization (WMO) definition of the tropopause, it was determined that of the 333 aircraft for which flight level meteorological data could be determined, 225 were operating in the troposphere between FL 310 and 300 meters below the tropopause, and would therefore have been assigned a flight level relative humidity of 40 percent by the JETRAX algorithm because of the model's "40/70/10" relative humidity assumption. Likewise, the 49 aircraft observed operating within 300 meters above or below the tropopause would have been assigned a relative humidity of 70 percent, and the 59 aircraft operating in the stratosphere more than 300 meters above the tropopause would be assumed by JETRAX to be flying in conditions of 10 percent relative humidity. As a general rule, the *in situ*

relative humidities measured by the radiosondes were considerably lower than those assumed by JETRAX.

Of the 397 positively identified aircraft, 186 (47 percent) were observed to be producing contrails, while the other 211 (53 percent) were not producing contrails. For the 333 observations paired with meteorological data, flight level temperatures ranged from - 66.1 to - 36.9 degrees Celsius and relative humidities ranged from 1 to 54 percent. The distribution of flight levels and temperatures for these 333 aircraft observations is plotted in Figure 7:

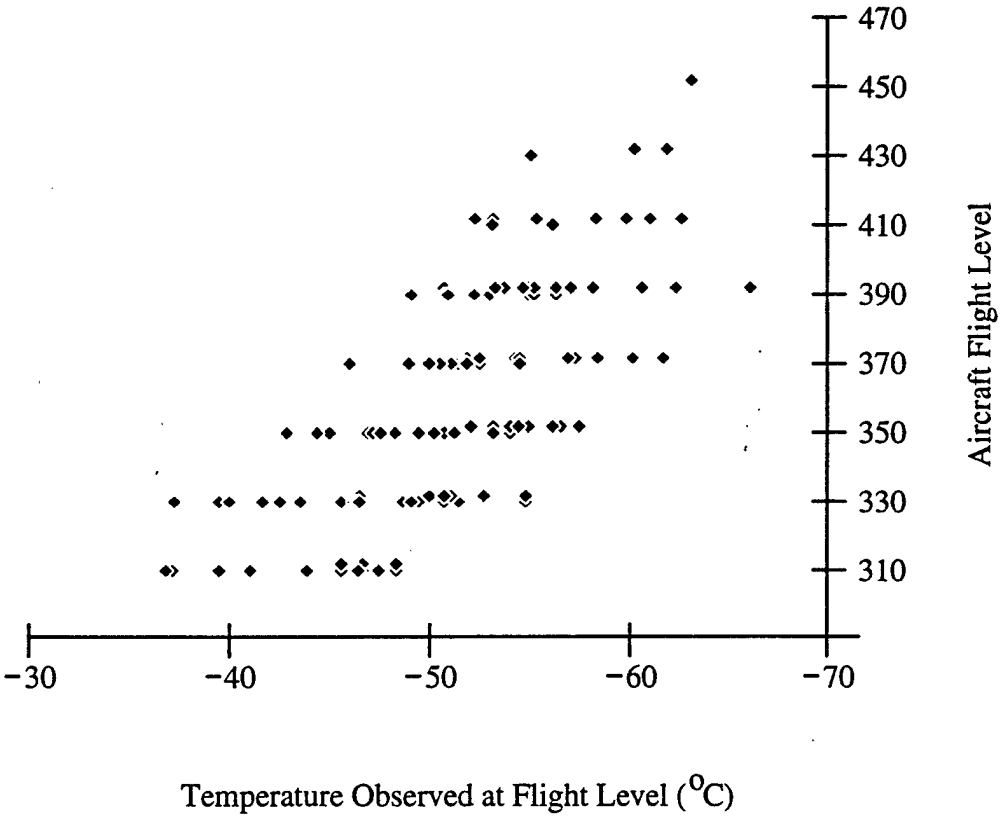

Fig 7. Distribution of Temperatures and Flight Levels of Observed Aircraft

A summary of each day's average observed flight level conditions is shown in Table 8, while all individual aircraft observations are included in Appendix C.

Table 8. Observed Flight Level Conditions

Date	Sample Size	Mean Flight Level	Mean Ambient Pressure (mb)	Mean Ambient Temp (C)	Mean Ambient RH (%)	Average Assumed [40/70/10] RH (%)	Aircraft Producing Contrails (%)	Tropo-pause Height (mb)
All Days	333	354.9	234.7	-51.2	17.3	39.1	48.7	285.5
18-Sep-97	19	370.0	217.3	-53.8	14.3	54.2	52.6	204.4
19-Sep-97	1	350.0	238.0	-47.0	45.0	40.0	100.0	N/A
24-Sep-97	8	342.5	247.8	-46.6	11.6	40.0	0.0	145.8
25-Sep-97	9	350.0	238.8	-42.1	2.8	40.0	0.0	N/A
01-Oct-97	37	357.6	231.1	-51.4	6.1	36.8	70.2	246.4
02-Oct-97	20	341.0	249.8	-50.1	39.2	40.0	45.0	N/A
04-Oct-97	10	378.0	209.9	-53.6	8.1	40.0	20.0	133.5
05-Oct-97	4	365.0	223.2	-48.0	8.5	40.0	50.0	116.5
06-Oct-97	14	374.3	214.1	-52.1	13.3	40.0	42.9	127.1
10-Oct-97	25	345.2	246.1	-48.8	7.0	40.0	24.0	158.6
12-Oct-97	13	340.8	250.2	-43.9	37.2	40.0	0.0	110.7
13-Oct-97	8	340.0	250.7	-43.3	40.3	40.0	0.0	106.8
14-Oct-97	18	354.4	235.7	-46.8	22.0	40.0	5.6	148.5
15-Oct-97	31	358.4	231.3	-50.5	7.4	37.1	3.2	232.2
16-Oct-97	11	353.6	235.6	-53.2	18.0	45.5	45.5	245.0
17-Oct-97	6	330.0	261.9	-49.0	4.0	45.0	0.0	247.7
21-Oct-97	10	378.0	209.5	-55.2	9.3	28.0	100.0	234.4
22-Oct-97	12	363.3	224.8	-53.9	7.9	20.0	91.7	270.0
28-Oct-97	19	363.9	225.5	-56.5	24.2	43.2	94.7	191.4
29-Oct-97	28	340.7	251.2	-54.4	27.4	38.9	96.4	199.8
30-Oct-97	30	355.3	234.0	-55.0	25.4	36.0	93.3	220.3

4.1.2 Aircraft Based Observation Data

4.1.2.1 High Bypass Engine Type (C-141) Observations

Flight testing of the Interim Operational Capability Lidar was conducted from 30 September through 3 October 1997, and again during the third and fourth weeks of December. During the first set of flights, for various reasons, an altitude conducive to contrail formation was reached only once, on Friday 3 October. Flying in the Buckeye Military Operations Area (MOA) in south-central Ohio, a steady spiral climb was conducted from FL 200 to FL 410. The JETRAX model's 1800Z forecast for this area predicted a contrail base of 38,000 feet, and the onset of contrail formation was observed at 1820Z at an altitude of 40,600 feet. The system test on 23 December 1997 consisted of a cross-country flight approximately three hours in length across much of the Mid-Atlantic and Appalachian regions. The JETRAX model had predicted a contrail base of 29,000 feet at 1800Z for the area in which observations were attempted. Unfortunately, air traffic controllers at the FAA's Indianapolis Center were only able to grant a clearance up to 31,000 feet to our aircraft, but in straight and level flight at that altitude the onset of contrail formation had not yet begun. Contrails were being produced by numerous commercial aircraft at flight levels that appeared to be just above that of our C-141, perhaps at FL 330 or FL 350, but neither the author, the aircraft commander, nor the Wright Laboratory Test Director saw contrails being produced by our aircraft. Though the exact base of the contrail layer was not observed on this day, it is interesting to note that on neither of the flights did the onset of contrail formation occur at an altitude below

that which was forecast. It has been proposed in the past that the algorithm used by AFGWC had an inherent high forecast base bias (Rabayda, 1997), but that was before JETRAX began ingesting NOGAPS data. Though a sample size of two observations is certainly not a statistically significant basis for drawing any conclusions, a "low" forecast bias, if anything, was observed on both flights. On both occasions the JETRAX forecast predicted that contrails would begin to occur at a lower flight level than that where the bases were observed.

4.1.2.2 Low Bypass Engine Type (F-16) Observations

The 178th Fighter Wing based at Springfield, Ohio was conducting training in primarily low altitude air-to-ground missions throughout the first half of October, so the opportunity to attempt contrail observations was not available until air-to-air training resumed later in the month. The dates that observations were made and the corresponding JETRAX forecast for the base of the contrail level are shown in Table 9.

Table 9. F-16 Observations of Contrail Formation Onset

Date	JETRAX Forecast	F-16 Observation
23-Oct-97	31,000	31,700
25-Oct-97	35,000	35,500
28-Oct-97	35,000	34,500
29-Oct-97	32,000	33,000
30-Oct-97	36,000	34,000
31-Oct-07	37,000	31,000*
1-Nov-97	no	33,000*

All F-16 observations were accomplished in the Buckeye MOA. As indicated in Table 9, the JETRAX low bypass forecasts compared very favorably to what the F-16 pilots observed. The observations from 31 October and 1 November are marked with an asterisk (*) because on both days the pilots reported that the contrails they observed were very faint and only occurred through an altitude layer that was about 1,000 to 1,500 feet thick. The pilots that flew the mission on 1 November continued to climb to an altitude of about 40,000 feet but did not see any further contrail development. The JETRAX model forecast could have been correct on either of these days because it discards any contrail layers that are not at least 2,000 feet thick. As with the high bypass engine observations made from the C-141, the sample size of the low bypass F-16 observations is far too small to draw any meaningful conclusions. However, based only on these observations, a high forecast base bias is not readily apparent.

4.2 Data Analysis

4.2.1 Measures of Accuracy

A measure of accuracy is a statistical tool which is used to determine the average agreement between forecasting an event and that event actually occurring (Wilks, 1995:236). Several such tools can make use of data from 2 x 2 contingency tables and provide some measurement of the accuracy of categorical "yes/no" forecasts.

4.2.1.1 Hit Rate

The Hit Rate (H) is a basic measure of accuracy. It represents the fraction of n number of forecasting opportunities where the forecast method correctly predicts the observed event. The Hit Rate, or proportion correct, is calculated as follows:

$$H = \frac{a + d}{n} \tag{22}$$

where

H = Hit Rate

a = number of events where contrails were forecast and observed

d = number of events where contrails were not forecast and not observed

n = sample size of all observations

The Hit Rate credits correct "yes" and "no" forecasts with equal weight, and also penalizes incorrect forecasts equally. The best possible Hit Rate is one and the worst possible Hit Rate is zero (Wilks, 1995:240).

4.2.1.2 Critical Success Index

Another frequently used measure of accuracy is the Critical Success Index (CSI), which considers only those events where contrails were forecast (all a and b entries in the contingency table) or observed (all c entries). As such, it may be considered as the Hit Rate once all the correct "no" forecasts (d entries) have been removed from consideration. Also referred to as the Threat Score, the Critical Success Index is computed as follows:

$$CSI = \frac{a}{a + b + c} \tag{23}$$

where

CSI = Critical Success Index

a = number of events where contrails were forecast and observed to occur

b = number of events where contrails were forecast but not observed to occur

c = number of events where contrails were not forecast but were observed to occur

The CSI is particularly effective when the number of "yes" forecasts is substantially lower than the number of "no" forecasts. Like the Hit Rate, the best possible CSI is one, and the worst possible CSI is zero (Wilks, 1995:240).

4.2.1.3 False Alarm Rate

The False Alarm Rate (FAR) gives the proportion of those events that were forecast but did not occur. The FAR is computed as:

$$FAR = \frac{b}{a + b} \tag{24}$$

The False Alarm Rate differs from the other statistical measures of accuracy in that a low FAR value indicates higher accuracy. The best possible FAR is zero and the worst possible FAR is one (Wilks, 1995:240-241).

4.2.2 Measure of Bias

The Bias Ratio (B) for categorical forecast methods is a comparison of the average forecast with the average observation. It is simply the ratio of the number of "yes" forecasts to the number of "yes" observations. The Bias Ratio is given by:

$$B = \frac{a + b}{a + c} \tag{25}$$

A perfectly unbiased forecast method would predict the event the same number of times the event occurred, resulting in a Bias Ratio of one. A Bias Ratio greater than one results when the event was forecast more often than observed and indicates that the event was overforecast. Conversely, a Bias Ratio of less than one means that the event was underforecast. Since the Bias Ratio says nothing about the correspondence between the forecasts and observations of the event on particular occasions, it is not a measure of accuracy.

4.2.3 Measures of Skill

Forecast skill scores measure the relative accuracy of a set of forecasts, based on a set of standard reference forecasts. Skill scores are expressed as a percentage improvement over the set of reference forecasts. Therefore, any skill score greater than zero shows an improvement over the set of reference forecast technique, while a skill score less than zero indicated poorer skill. A skill score exactly equal to zero indicates that the proposed forecast technique is equal in skill to the reference technique.

4.2.3.1 Heidke Skill Score

The Heidke Skill Score HSS is based on the Hit Rate as the basic accuracy measure. The reference accuracy measure in the Heidke score is the Hit Rate that would be achieved by random forecasts, subject to the constraint that the marginal distributions of the randomly generated forecasts and observations are the same as those of the actual verification data set. Perfect forecasts receive Heidke scores of one, forecasts equivalent to the reference forecasts receive an HSS of zero, and negative scores are assigned to forecasts that are worse than the reference forecasts. The Heidke Skill Score is given by:

$$HSS = \frac{2\,(ad - bc)}{(a + c)(c + d) + (a + b)(b + d)} \qquad (26)$$

4.2.3.2 Kuipers Skill Score

The Hanssen-Kuipers Discriminant or Kuipers Skill Score (KSS) gives an "impartial and satisfactory" indication of forecast skill for scientific purposes (Bjornson, 1992:10). Random forecasts, constrained to be unbiased, serve as the reference forecast technique in the KSS. Therefore, the hypothetical reference forecasts have a probability distribution equal to the climatology of the sample. Consequently, the probability of forecasting contrails equals the probability of observing contrails, and the probability of not forecasting contrails equals the probability of not observing contrails (Wilks, 1995:249). The Hanssen-Kuipers Discriminant is calculated as follows:

$$KSS = \frac{ad - bc}{(a + c)(b + d)} \tag{27}$$

4.2.4 Measures of Statistical Significance

For the statistical measures of accuracy, bias, and skill to be meaningful, it must be shown that there is a connection or association between the column classification in a contingency table (contrail observed) and the row classification (contrail forecast). Otherwise, an apparently good relationship between observing contrails when they are forecast (a large count for entry "a" in the contingency table) may simply be due to chance. In order to show such a relationship between the row and column classifications (significance) exists, a test of independence must be performed.

Two events are independent if the probability of Event B occurring, given that Event A has already occurred, is equal to the probability of Event B occurring alone (Devore, 1995:79). Applied to contingency tables, the probability of observing a contrail, given that a contrail was forecast, equals the probability of observing a contrail regardless of the forecast. Dependence between columns and rows must be demonstrated for the data to be deemed statistically significant.

To show dependence in the contingency tables, they were entered into the STATISTIX analytical software package so that the Pearson chi square test could be conducted with a level of significance of one percent. If the P-value computed in the test was less than 0.01, the notion of independence was rejected and the contrail condition observed was declared dependent upon the forecast category. At a one percent level of significance,

there is only a 1 out of 100 probability that the forecast was correctly made by chance. Results of the Pearson chi square tests and P-values for each subset of the observation data is presented in Tables 10, 11, and 13 in Chapter 5.

5. Findings and Conclusions

5.1 Results

5.1.1 JETRAX Validation

A total of 397 ground based contrail observations were collected and used to measure the accuracy of AFWA JETRAX contrail forecast products issued on 27 different days between 18 September and 31 October 1997. Contingency tables were constructed as described in Chapter 3, and the statistical measures of accuracy, bias, and skill described in Chapter 4 were applied. Separate contingency tables were constructed for 30-hour forecasts, 24-hour forecasts, 18-hour forecasts, forecasts for high bypass engine types, forecasts for low bypass engine types, forecasts made on the "driest" days with an average observed flight level relative humidity of less than 10 percent, forecasts on "moist" days with an average observed flight level relative humidity of greater than 20 percent, and finally for all forecasts. Though the criteria for discerning "moist" days form "driest" days may seem somewhat arbitrary, it is roughly equivalent to one half of one standard deviation above the mean relative humidity or higher for "moist" days and one half of one standard deviation below the mean relative humidity or lower for the "driest" days. This convention also yielded similar sample sizes for the two categories, designating 137 observations as having been taken on moist days and 144 on dry days. The data set was also split into those observations taken on days where the average flight level relative

humidity was greater than 20 percent and days where it was less than 20 percent so that all observations would be included. In addition, verification statistics were also calculated for persistence and climatology. Monthly climatological contrail probabilities were obtained for Dayton's latitude and longitude from the Air Force Combat Climatology Center (AFCCC) via their internet home page at http://thunder.scott.af.mil/, and flight levels for which the probability of contrails was 70 percent or greater were considered to be levels at which contrails were expected to form. Persistence is taken to be "yesterday's forecast" applied to "today's observations", the JETRAX forecast for contrail bases and tops that was valid 24 hours prior to the time the observations under consideration were taken. Each of the eleven contingency tables described above were determined to be statistically significant, and the results are shown in Table 10 below.

Table 10. JETRAX Forecast Statistics
(Based on all 397 Aircraft Observations)

Forecast Description	Forecast Sample Size	Hit Rate (%)	Critical Success Index	FALSE Alarm Rate	Bias Ratio	Kuipers Skill Score	Pearson's Chi Squared	Pearson's P-Value
All Forecasts	816	84.4	0.715	0.152	0.967	0.6866	386.2	0.0000
30-hr Forecasts	280	81.8	0.671	0.188	0.977	0.6328	112.5	0.0000
24-hr Forecasts	262	83.2	0.669	0.127	0.850	0.6501	115.6	0.0000
18-hr Forecasts	274	88.3	0.797	0.137	1.058	0.7660	161.5	0.0000
High Bypass	588	82.8	0.746	0.151	1.014	0.6418	243.8	0.0000
Low Bypass	228	88.6	0.435	0.167	0.571	0.4547	75.1	0.0000
Moist Days (>20% RH)	302	91.4	0.863	0.035	1.500	0.8405	206.4	0.0000
Dry Days (<20% RH)	423	78.0	0.594	0.249	0.984	0.5508	128.9	0.0000
Driest Days (<10% RH)	308	76.0	0.565	0.232	0.887	0.5072	81.6	0.0000
Persistence	397	71.3	0.479	0.250	0.761	0.4063	71.4	0.0000
Climatology	397	72.0	0.587	0.344	1.296	0.4561	86.2	0.0000

The JETRAX algorithm generated correct predictions for 84.4 percent of all forecasts under study with a false alarm rate of 15.2 percent. The model performed exceptionally well under moist atmospheric conditions with a Hit Rate of 91.4 percent on days when the average observed flight level relative humidity was greater than 20 percent. That performance fell off to a 76 percent Hit Rate on the driest days where the average ambient relative humidity was less than 10 percent. With a Kuipers Skill Score of 0.6866, JETRAX demonstrated greater skill than both persistence (KSS = 0.4063) and climatology (KSS = 0.4561). The bias ratio of 0.967 for all forecasts, though very nearly an unbiased 1.0, indicates that contrails are slightly underforecast. This would mean that contrails are typically forecast less often than they are observed, which supports Rabayda's assertion that a high forecast base bias exists in the current AFWA forecast method. As one might expect, longer range forecasts demonstrated less accuracy than did shorter range forecasts. The 30-hour forecasts had a Hit Rate of 81.8 percent, which increased to 83.2 percent for 24-hour forecasts and rose again to 88.3 percent for 18-hour forecasts. Each of the nine subsets of the JETRAX forecast data demonstrated higher Hit Rates than did persistence (71.3 percent) or climatology (72.0 percent).

5.1.2 Schrader, Schumann, and Hanson Algorithm Validation

The same statistical tests were applied to the critical temperature formulations of three other contrail forecast algorithms. If the critical temperature calculated was colder than the ambient flight level temperature, contrails would be expected to form. Contingency tables were constructed in the same manner as previously described for both the *in situ*

relative humidity measured by the radiosonde and the assumed 40/70/10 relative humidity profile employed by the JETRAX algorithm. The sample size for the *in situ* and 40/70/10 cases is 333 aircraft observations. Of these 333 aircraft for which flight level relative humidity could be determined, 122 aircraft were observed to be operating in "moist" atmospheric conditions of 20 percent relative humidity or greater while 211 were flying through "dry" conditions where relative humidity was less than 20 percent. The results of several statistical measures of accuracy, bias, and skill are presented in Table 11:

Table 11: Schumann, Schrader, and Hanson Algorithm Validation Statistics
(Based on 333 the Observations for Which Radiosonde Data Were Available)

Forecast Algorithm	RH Profile	Hit Rate (%)	Critical Success Index	False Alarm Rate	Bias Ratio	Kuipers Skill Score	Pearson's Chi Squared	Pearson's P-Value
Schumann	in situ	81.4	0.668	0.167	0.926	0.625	131.4	0.0000
	40/70/10	77.2	0.627	0.247	1.049	0.545	98.7	0.0000
	moist	82.2	0.708	0.089	0.836	0.670	54.7	0.0000
	dry	80.6	0.643	0.213	0.989	0.607	77.8	0.0000
Schrader	in situ	79.0	0.630	0.185	0.901	0.577	112.4	0.0000
	40/70/10	77.5	0.631	0.243	1.043	0.550	100.8	0.0000
	moist	79.5	0.662	0.125	0.836	0.600	44.4	0.0000
	dry	78.7	0.609	0.222	0.947	0.560	68.0	0.0000
Hanson	in situ	63.7	0.253	0.000	0.253	0.253	49.4	0.0000
	40/70/10	71.5	0.500	0.228	0.759	0.423	63.8	0.0000
	moist	77.9	0.597	0.000	0.597	0.597	48.9	0.0000
	dry	55.5	0.011	0.000	0.011	0.011	1.2	0.2680

The Schumann algorithm had the highest Hit Rate in three of the four moisture profiles, performing consistently well under varying relative humidities. The fact that it demonstrated little variance in Bias Ratio indicates that the model does not tend to

consistently overforecast or underforecast contrail formation in response to changes in flight level humidity. The overall performance of the Schrader algorithm was comparable to that of Schumann. The Hanson algorithm, on the other hand, had the lowest Hit Rate in three of four humidity categories. The fact that the Hanson Hit Rate drops from 71.5 percent with the assumed 40/70/10 moisture profile to 63.7 percent when in situ measurements are used raises some question as to how physically representative of the atmospheric processes their algorithm actually is. Both the Schrader and Schumann models perform slightly better with real-time radiosonde moisture data than with the 40/70/10 profile.

Though the 71.5 percent Hit Rate of the Hanson algorithm for moist conditions is within 5 percent of both of the other algorithms, its Hit Rate plummets to 55.5 percent for low flight level relative humidities of less than 20 percent. By contrast, the Schumann Hit Rate dropped from 82.2 percent to 80.6 percent, while the Schrader Hit Rate only dropped from 79.5 percent to 78.7 percent for the same relative humidity criteria. Although the low False Alarm Rates exhibited by the Hanson algorithm are desirable, they are in this case merely a reflection of how infrequently it forecast contrails to occur. The extremely cold critical temperatures generated by the Hanson algorithm made it very unlikely for the occurrence of contrails to be predicted, as reflected in the fact that contrails were considerably underforecast for each flight level moisture category. The low Bias Ratios of 0.253 for *in situ* relative humidity measurements and 0.011 for dry flight level conditions clearly indicate that the Hanson algorithm has an extremely high forecast base bias as compared to the formulations of Schumann and Schrader.

5.2 Conclusions

5.2.1 Conclusions Drawn From JETRAX Validation Study

The Air Force Weather Agency is providing excellent contrail forecast products to its operational customers. With an overall Hit Rate of 84.4 percent and False Alarm Rate of 15.2 percent, no immediate changes to the algorithm seem warranted. The 30-hour forecasts are providing mission planners with information that is more than 80 percent accurate, while forecasters are briefing pilots with an 18-hour forecast that was shown to be nearly 90 percent accurate.

While the conclusion of Rabayda that the model has a high forecast base bias was supported by the overall Bias Ratio of 0.967, it is very nearly an unbiased 1.000 and provides little cause for concern. It was interesting to note, however, that on "moist" days with an average flight level relative humidity of 20 percent or greater, the JETRAX model had a Bias Ratio of 1.500, indicating that contrails were overforecast and a *low* forecast base bias was apparent under these conditions.

Though the sample size of the airborne observations was too small to draw any truly meaningful conclusions, a low forecast base bias was implied by both of the high bypass observations and three of the seven low bypass observations. Both of the high bypass forecasts were too low by at least 2,000 feet. The last two of the seven low bypass observations were questionable as to whether the criteria for visible moisture and vertical extent had been met. Removing these observation/forecast pairs from consideration, four of the of the remaining five contrail base forecasts for low bypass engine types were

within 1,000 feet of what was observed while the fifth was 2,000 feet too high. Again, with so few observations, a claim that the JETRAX forecast bases have been proven to be sufficiently accurate would simply not be statistically sound. The observations did however compare very favorably to the contrail bases that JETRAX had forecast.

5.2.2 Conclusions Drawn From Algorithm Comparison

Asbury asserted that the Hanson algorithm did not improve upon existing contrail forecast techniques under low relative humidity conditions as it had been claimed (Asbury, 1997:72). A data set that was both considerably larger and more evenly balanced between "yes" and "no" contrail observations was collected during the course of this research, but the conclusion remains unchanged. The Hit Rate of contrail forecasts generated by the Hanson algorithm was found to drop from a respectable 77.9 percent under moist atmospheric conditions to an unacceptable 55.5 percent for aircraft which were flying in dry atmospheric conditions of less than 20 percent. Since the Hanson algorithm failed to adequately predict contrails under all atmospheric conditions, it is not recommended for use by the Air Force Weather Agency.

Both the Schrader and Schumann algorithms correctly forecast the occurrence or nonoccurrence of contrails in approximately 80 percent of the cases observed. Both had slightly higher skill scores and Hit Rates for *in situ* relative humidity measurements than for the assumed 40/70/10 relative humidity profile, and slightly lower skill scores and Hit Rates for aircraft observed at "dry" flight level relative humidities of less than 20 percent than for aircraft operating in "moist" conditions of 20 percent relative humidity or greater.

Both had False Alarm Rates of less than 25 percent and a Critical Success Index of greater than 0.60 for all flight level relative humidity profiles.

5.3 Post Analysis

The JETRAX algorithm uses an assumed relative humidity profile and forecast temperatures, yet statistically outperformed similar algorithms using flight level humidity and temperature values obtained from near real-time radiosonde data. In an attempt to explain this finding, the verification statistics and input data were further examined.

The 40/70/10 assumption was shown by the radiosonde data to significantly overestimate the relative humidity of the air through which the observed aircraft were flying, as indicated in Table 12. Though this supports Rabayda's conclusion that more accurate moisture input would not yield more statistically accurate forecasts, the fact remains none the less counterintuitive.

Table 12. Relationship Between Assumed and Observed Flight Level Humidity

	Troposphere	Within 300m of Tropopause	Stratosphere
Number of Observations	225	49	59
Assumed Relative Humidity	40%	70%	10%
Average Observed RH	21.2%	14.1%	4.7%
Max Observed RH	54%	31%	16%
Min Observed RH	1%	3%	1%
Standard Deviation	13.8%	7.3%	4.2%
Difference Between Assumed and Average Observed RH	(+) 18.9%	(+) 55.9%	(+) 5.3%

The similar algorithms of Schrader and Schumann both showed a slight drop in skill and accuracy when the radiosonde humidity data was replaced with the 40/70/10 profile. The typically higher humidity values of the assumed profile also caused the Bias Ratios of the Schrader and Schumann algorithms to increase from slightly less than one (underforecasting) to slightly greater than one (overforecasting). This finding is not counterintuitive. Higher humidity *should* make contrail formation more likely when all other factors remain unchanged. The fact that JETRAX uses higher humidity values than those typically observed does not, however, explain its superior performance to the similar algorithms, particularly when the performance of the other algorithms *decreased* when they used the same 40/70/10 profile.

The observation data was again reexamined to try to explain why JETRAX outperformed the other similar algorithms. The JETRAX validation was based on 397 visual aircraft observations, while the Schrader and Schumann algorithms could only produce critical temperature forecasts for those 333 observations which had corresponding flight level temperature and relative humidity data available. The 64 aircraft observations for which there was no corresponding radiosonde data were therefore removed from the full JETRAX validation data set. This effectively removed 114 correct and only 11 incorrect JETRAX forecasts from consideration. Some of the results from Table 10 (JETRAX Forecast Statistics) and Table 11 (Schumann, Schrader, and Hanson Algorithm Validation Statistics) are presented again in Table 13 so that the effect of removing these observations from consideration can be more directly viewed.

Table 13. Revised Statistical Comparison
(Full: Results Based On All Available Observations; Reduced: Observations For Which No Radiosonde Data Were Available Were Removed From Consideration; DBRITE: Only Observations Taken From the Wright-Patterson ATC Tower Were Considered)

Forecast Description	Data Set	Forecast Sample Size	Hit Rate (%)	Critical Success Index	False Alarm Rate	Bias Ratio	Kuipers Skill Score	Pearson's Chi Squared
All JETRAX Forecasts	Full	816	84.4	0.715	0.152	0.967	0.6866	386.2
	Reduced	691	83.2	0.710	0.145	0.943	0.6652	306.1
	DBRITE	593	78.6	0.517	0.28	0.900	0.5092	162.0
30-hr JETRAX Forecasts	Full	280	81.8	0.671	0.188	0.977	0.6328	112.5
	Reduced	241	80.9	0.664	0.180	0.949	0.6165	92.1
	DBRITE	207	77.8	0.516	0.279	0.895	0.4997	54.4
24-hr JETRAX Forecasts	Full	262	83.2	0.669	0.127	0.850	0.6501	115.6
	Reduced	233	82.0	0.664	0.117	0.825	0.6356	97.7
	DBRITE	204	76.0	0.479	0.262	0.782	0.4499	46.5
18-hr JETRAX Forecasts	Full	274	88.3	0.797	0.137	1.058	0.7660	161.5
	Reduced	217	87.1	0.797	0.134	1.050	0.7320	118.2
	DBRITE	182	82.4	0.568	0.300	1.070	0.6071	64.7
High Bypass JETRAX Forecasts	Full	588	82.8	0.746	0.151	1.014	0.6418	243.8
	Reduced	494	81.7	0.744	0.146	0.997	0.6110	185.1
	DBRITE	398	75.1	0.564	0.293	1.040	0.4990	97.1
Low Bypass JETRAX Forecasts	Full	228	88.6	0.435	0.167	0.571	0.4547	75.1
	Reduced	194	87.1	0.444	0.130	0.548	0.4565	65.6
	DBRITE	195	85.6	0.222	0.000	0.222	0.2222	36.8
Schumann Algorithm	in situ	333	81.4	0.668	0.167	0.926	0.6254	131.4
	40/70/10	333	77.2	0.627	0.247	1.049	0.5445	98.7
Schrader Algorithm	in situ	333	79.0	0.630	0.185	0.901	0.5767	112.4
	40/70/10	333	77.5	0.631	0.243	1.043	0.5504	100.8

A Pearson's Chi Square test was conducted to ensure the statistical significance of each subset of the data. Since every case returned a P-value of 0.0000, the P-values were not included in Table 13. Significance is assumed.

Results from both the original and modified JETRAX verification data sets are grouped such that direct comparisons can be made. The smaller data sets from which the

observations with no available sounding data were removed generally exhibited about a one percent lower hit rate than did the full data sets, but they were still more accurate than the Schumann and Schrader algorithms. The difference in the observation data sets failed to fully explain the skill and accuracy discrepancies between the JETRAX verification statistics and those of the other two similar algorithms.

While each observation could be compared to two or even three different JETRAX forecasts, it could be used to generate only one critical temperature "nowcast" by the other algorithms. If more of the JETRAX forecasts were right than wrong, which was the case, then this could explain why JETRAX had higher Hit Rates in the "All JETRAX Forecasts" category. It does not explain, however, why the 18, 24, and 36 hour forecast statistics were better than those of the other two algorithms. Each of these results involved comparing each observation to only one forecast as well. One would have to go out to the 30-hour point, more than one day in advance, to find the point where the accuracy of the JETRAX contrail forecast products first drop to a level comparable to that of the other algorithms which used real-time temperature and relative humidity data.

The final subset of JETRAX forecasts examined were those compared only to the set of observations collected with the aid of the DBRITE radar scope and Flight Data System in the Wright-Patterson air traffic control tower. These observations comprised the subset least likely to be skewed in any way because the radar is equally likely to "see" all aircraft, whether they are producing contrails or not. There were 91 observations collected without the use of the radar, for which flight levels were attained solely from the FAA flight log from the corresponding time periods. Though fewer than ten of these

observations were typically made on any given day, they still accounted for nearly a quarter of the total. The overwhelming majority of these translated into correct forecasts of the occurrence of contrails, or "a" entries in the contingency tables. These observations were removed from consideration, and forecast statistics for the remaining observations which were made with the tower equipment appear in the rows of Table 13 labeled "DBRITE".

The JETRAX forecast Hit Rate for the "DBRITE" observations was 78.6 percent, which falls between the Hit Rates for the "*in situ*" and "40/70/10" categories of both the Schrader and Schumann algorithms. The fact that so many of the observations made without the use of the DBRITE were of correctly forecast "conning" aircraft explains, at least in part, why JETRAX statistically outperformed other similar algorithms.

5.4 Recommendations for Further Research

The modified observation method of Asbury can be implemented at any location where access to an air traffic control radar is available. The use of the DBRITE scope and Flight Data System to locate and identify airborne aircraft reduces the likelihood of collecting a data set that is skewed in favor of a larger number "yes" than "no" contrail observations. This is due to the fact that the radar is equally likely to detect all aircraft, conning or not. Virtually 100 percent of overflying aircraft were able to be positively identified using the ATC equipment, as compared to the approximately 65 percent which Asbury was able to positively identify with ground based observations and FAA records

alone. The use of a telescope in conjunction with the radar is also recommended so that the aircraft type can be confirmed visually as well.

The airborne contrail observations taken during this research were not nearly of a statistically significant sample size, but the accuracy of the forecast contrail bases is still nonetheless of vital interest during air combat operations. The JETRAX output was shown to be quite accurate on a yes/no basis, but determining how accurate its forecasts are for the exact bases of the contrail level would require much more extensive research.

There have been a large number of studies conducted in 1996 and 1997 that focused on the environmental impact of contrails, including the NASA-Ames Research Center SUCCESS program, research conducted by Dr. Kenneth Sassen at the University of Utah, a joint study between the NASA-Langley Research Center and the Air Force, and several papers by Dr. Ulrich Schumann. Efforts in this area are certain to continue.

The Schumann algorithm is unique in that it takes aerodynamic effects on the contrail formation process into consideration. Factors such as thrust, true air speed, and fuel flow go into the calculation of Schumann's propulsion efficiency. Average values of these variables were used in computing the propulsion efficiency for the high bypass and low bypass engine types considered in this study. One possible follow-on to this research could be to add more contrail observations to the existing data set and use aircraft specific values instead of average values in the propulsion efficiency calculations. Since Schumann combines classic mixing cloud theory with the effects of engine performance and aerodynamic drag, his method may well be proven to provide the most complete physical representation of the contrail formation process.

Appendix A. Saturation Vapor Pressure Calculation Using the Goff-Gratch Equation

The JETRAX algorithm uses a form of the Goff-Gratch equation shown below to determine whether a temperature forecast for a level in the atmosphere is colder than the critical temperature required for saturation and therefore contrail formation.

Temperature (T) must be entered in Kelvin (K), and the resulting value of the saturation vapor pressure (e_s) is in millibars. A plot of saturation vapor pressure versus temperature is shown in Figure A1.

$$GG1 = 23.832241$$

$$GG2(T) = 5.02808 \cdot \log(T)$$

$$GG3 = 1.3816 \cdot 10^{-7}$$

$$GG4(T) = 10^{(11.334 - 0.0303998 \cdot T)}$$

$$GG5 = 8.1328 \cdot 10^{-3}$$

$$GG6(T) = 10^{\left(3.49149 - \frac{1302.8844}{T}\right)}$$

$$GG7(T) = \frac{2949.076}{T}$$

$$e_s(T) = 10^{[GG1 - GG2(T) - GG3 \cdot GG4(T) + GG5 \cdot GG6(T) - GG7(T)]}$$

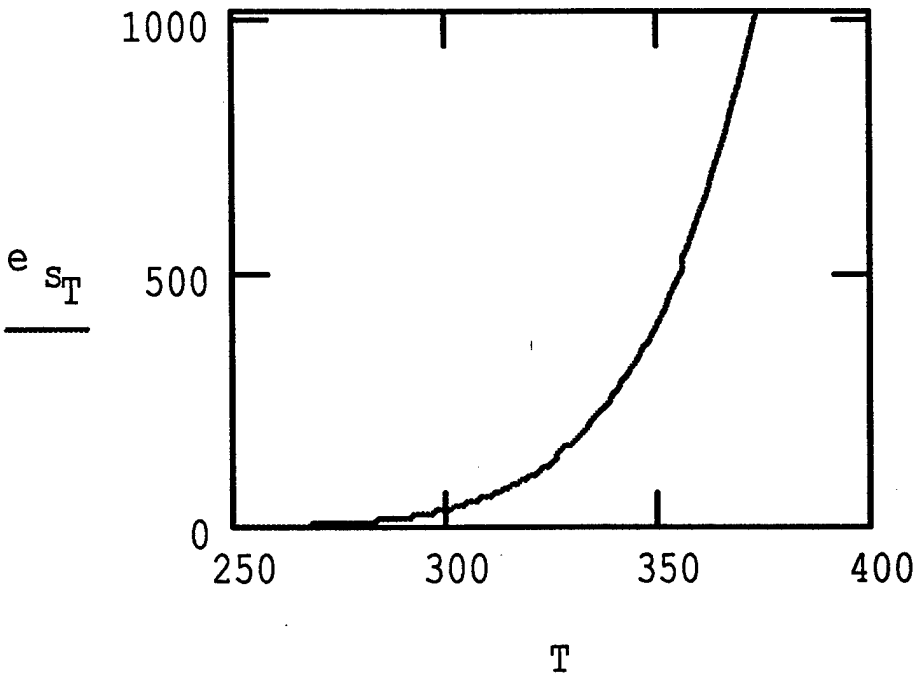

Fig A1. Plot of Saturation Vapor Pressure vs. Temperature

Appendix B. Radiosonde Comparison

On the morning of 9 October, a Vaisala RS80 model radiosonde was launched simultaneously with a radoisonde manufactured by Atmospheric Instrumentation Research, Inc. (AIR). The sounding data received from the two radiosondes was compared to that from the radiosonde lauched by the National Weather Service Office in Wilmington, Ohio, at approximately the same time. Each of the temperature and moisture profiles are shown on the next two pages in Figure B1 and Figure B2 respectively. The three temperature soundings were nearly identical. A difference can be seen, however, between the AIR and Vaisala dewpoint traces and that of the Wilmington sounding. The National Weather Service sounding has a much smoother dewpoint trace, where the greater resolution of the research quality radiosondes is readily apparent.

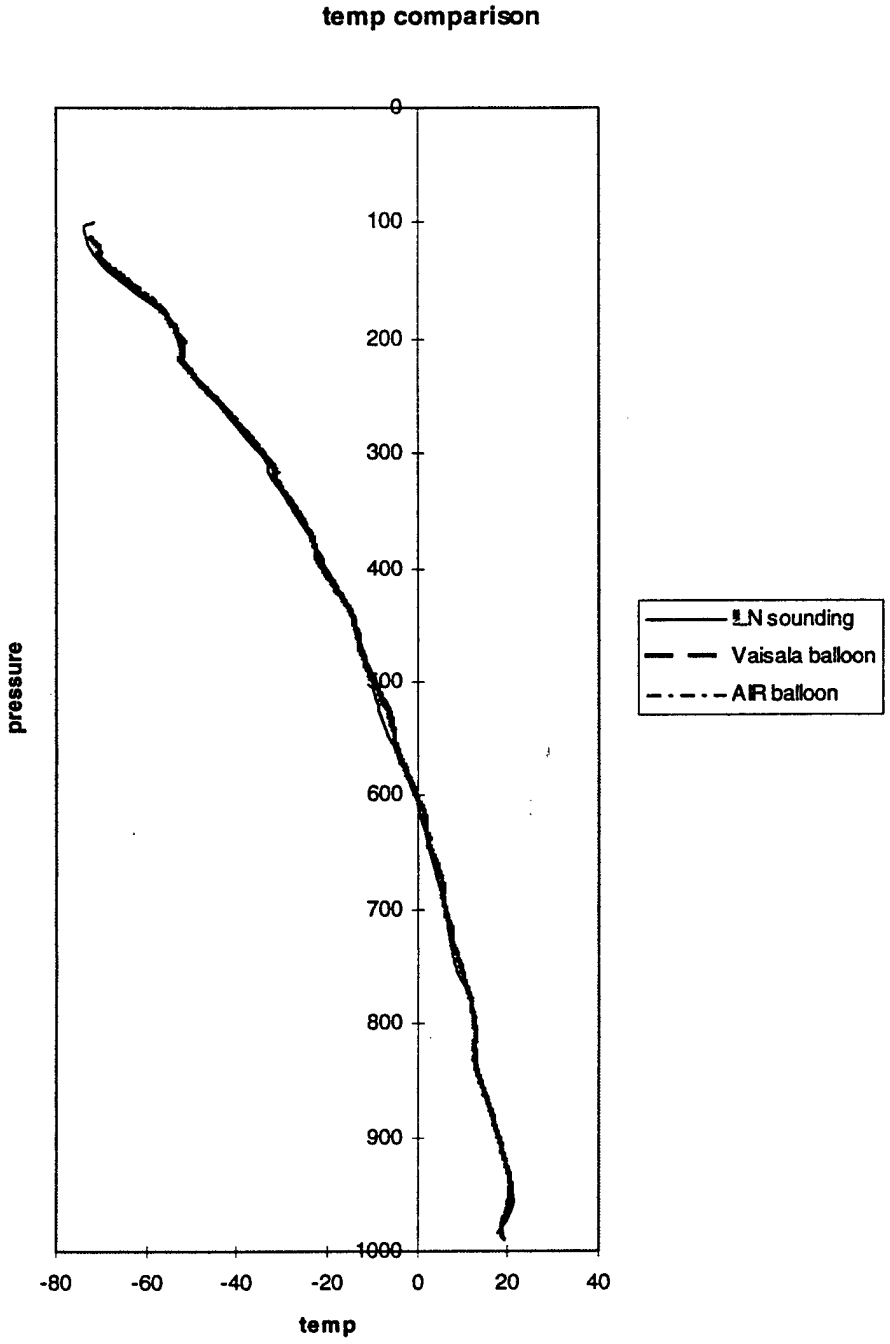

Fig B1. Comparison of Radiosonde Temperature Data

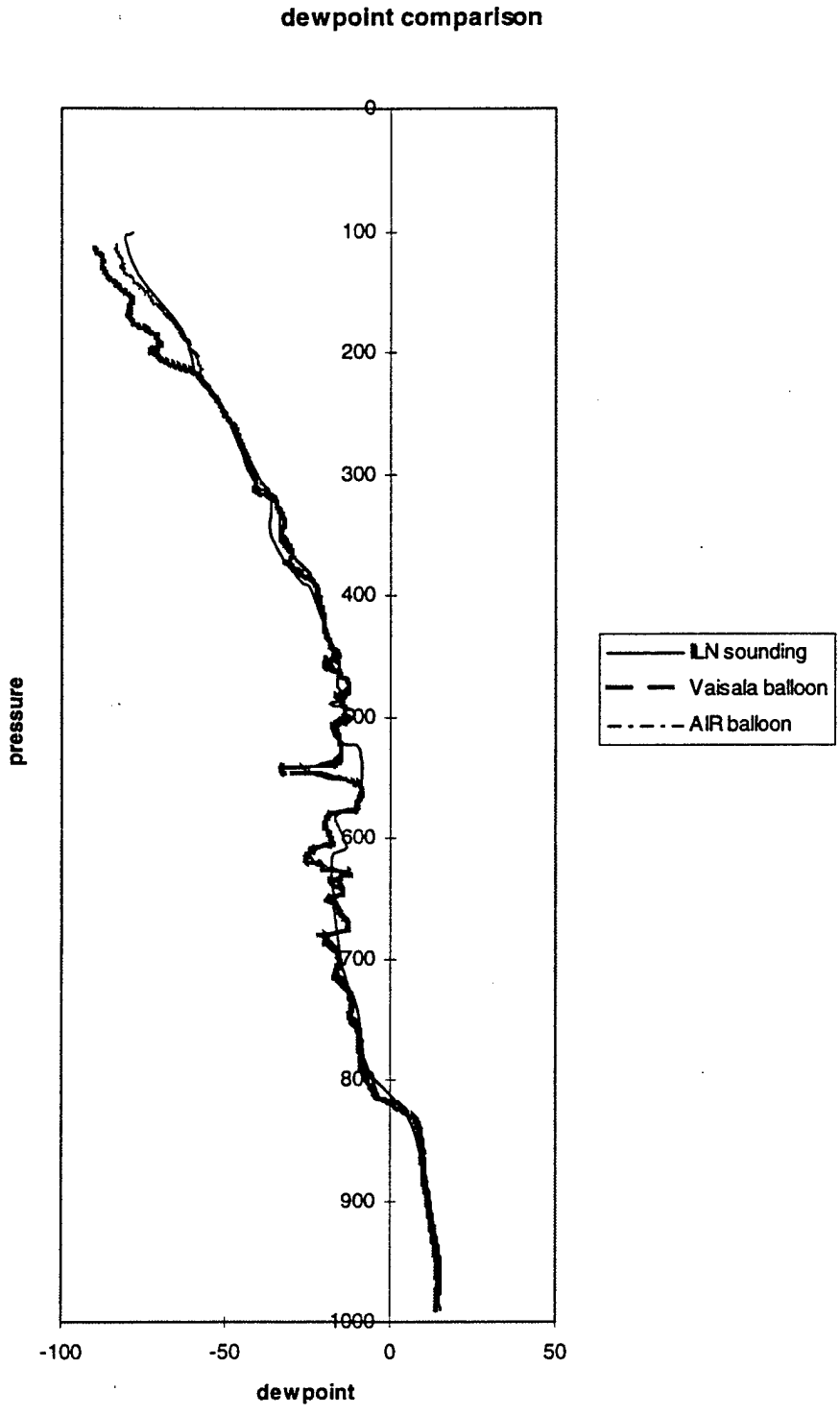

Fig B2. Comparison of Radiosonde Dewpoint Data

Appendix C: Ground Based Contrail Observations

The daily aircraft observations made at Wright-Patterson Air Force Base in conjunction with this forecast study are presented. Each table contains the call sign, aircraft type, engine bypass ratio category, and flight level of each observed aircraft, as well as whether or not a contrail was observed, the flight level meteorological conditions of pressure in millibars, temperature in degrees Celsius, and percent relative humidity as determined from radiosonde data, and finally the assumed relative humidity that the JETRAX algorithm would have assigned to each particular aircraft based on the aircraft's altitude in relation to the tropopause. Missing data, indicated by the letter "M", was usually the result of the loss of the radiosonde signal before data could be recorded.

Table C1. Observations From 18 September 1997

Call Sign	Type	Engine	FL	Observed	Pressure	Temp	In Situ RH	Model RH
TWA29	MD-80	Low	350	no	238.0	-51.4	17	40
NWA1553	DC-9	Low	350	no	238.0	-51.4	17	40
TWA523	B727	Low	350	no	238.0	-51.4	17	40
NWA1578	DC-9	Low	330	no	261.6	-46.5	22	40
USA204	B737-F	High	350	no	238.0	-51.4	17	40
COA1137	B737-S	High	350	no	238.0	-51.4	17	40
DAL1429	B757	High	350	no	238.0	-51.4	17	40
N1549W	BE-40	High	390	no	196.5	-56.3	11	70
UPS9260	DC8-S	High	370	yes	216.3	-54.7	16	40
N900MA	DA-90	High	390	yes	196.5	-56.3	11	70
UAL89	B757	High	390	yes	196.5	-56.3	11	70
TWA15	B767	High	390	yes	196.5	-56.3	11	70
N1UP	C-650	High	370	yes	216.3	-54.7	16	40
AAL517	MD-80	Low	350	no	238.0	-51.4	17	40
UAL8151	B767	High	390	yes	196.5	-56.3	11	70
ACA691	EA-32	High	390	yes	196.5	-56.3	11	70
ACA825	EA-33	High	390	yes	196.5	-56.3	11	70
TWA417	B757	High	390	yes	196.5	-56.3	11	70
UAL9	B767	High	390	yes	196.5	-56.3	11	70

Table C2. Observations From 19 September 1997

Call Sign	Type	Engine	FL	Observed	Pressure	Temp	In Situ RH	Model RH
TWA29	MD-80	Low	350	no	238.0	-47.0	45	40
N90CN	C-650	High	390	yes	196.5	M	M	M
N910S	G4	High	430	yes	197.5	M	M	M
UPS2053	B767	High	390	yes	196.5	M	M	M
N211FX	LR-60	High	390	yes	197.5	M	M	M

Table C3. Observations From 22 September 1997

Call Sign	Type	Engine	FL	Observed	Pressure	Temp	In Situ RH	Model RH
UAL493	B757	High	390	yes	196.5	M	M	M
AAL1345	MD-80	Low	310	no	287.0	M	M	M
AAL1431	B757	High	390	yes	196.5	M	M	M
UPS2955	DC8-S	High	370	yes	216.3	M	M	M
N836MF	G2	High	430	yes	162.3	M	M	M
ACA691	EA-32	High	390	yes	196.5	M	M	M
TWA399	B757	High	390	yes	196.5	M	M	M
COA195	B727	Low	330	no	261.6	M	M	M
TWA417	B757	High	390	yes	196.5	M	M	M
TWA37	B757	High	390	yes	196.5	M	M	M
AAL1806	B757	High	370	yes	216.3	M	M	M

Table C4. Observations From 23 September 1997

Call Sign	Type	Engine	FL	Observed	Pressure	Temp	In Situ RH	Model RH
COA1260	B737-J	High	370	yes	216.3	M	M	M
NWA955	B727	Low	330	no	261.6	M	M	M
AAL1806	B757	High	410	yes	178.6	M	M	M
USA21	B757	High	350	yes	238.0	M	M	M
NWA489	DC-9	Low	330	no	261.6	M	M	M
USA2298	B737	High	370	yes	216.3	M	M	M

Table C5. Observations From 24 September 1997

Call Sign	Type	Engine	FL	Observed	Pressure	Temp	In Situ RH	Model RH
DAL27	MD-11	High	370	no	216.3	-51.1	11	40
SWA351	B737-S	High	350	no	238.0	-48.3	14	40
VJA249	DC-9	Low	350	no	238.0	-48.3	14	40
COA1237	DC-9	Low	310	no	287.0	-41.2	11	40
COA1995	MD-80	Low	350	no	238.0	-48.3	14	40
NWA47	B757	High	370	no	216.3	-51.1	11	40
USA434	DC-9	Low	310	no	287.0	-41.2	11	40
NWA531	DC-9	Low	330	no	261.6	-43.6	7	40

Table C6. Observations From 25 September 1997

Call Sign	Type	Engine	FL	Observed	Pressure	Temp	In Situ RH	Model RH
UAL350	B737-S	High	350	no	238.0	-42.9	3	40
N424CR	BE-20	High	350	no	238.0	-42.9	3	40
UPS2133	B757	High	350	no	238.0	-42.9	3	40
SWG503	DC-9	Low	330	no	261.6	-37.3	1	40
UAL976	B767	High	350	no	238.0	-42.9	3	40
N600RE	CL-60	High	370	no	216.3	-46.1	4	40
TWA176	B727	Low	330	no	261.6	-37.3	1	40
TWA192	MD-80	Low	330	no	261.6	-37.3	1	40
TWA399	B757	High	390	no	196.5	-49.1	6	40

Table C7. Observations From 29 September 1997

Call Sign	Type	Engine	FL	Observed	Pressure	Temp	In Situ RH	Model RH
SWG503	DC-9	Low	330	no	261.6	M	M	M
USA1764	DC-9	Low	330	no	261.6	M	M	M
N71NK	C-560	High	390	no	196.5	M	M	M
N29WE	C-560	High	390	no	196.5	M	M	M
USA1193	B737	High	310	no	287.0	M	M	M
N30JD	C-550	High	330	no	261.6	M	M	M
AAL517	MD-80	Low	310	no	287.0	M	M	M
COA1297	B737	High	350	no	238.0	M	M	M
N805GT	C-650	High	370	no	216.3	M	M	M
DAL464	B767	High	410	no	178.6	M	M	M
NWA262	B727	Low	330	no	261.6	M	M	M
TWA430	MD-80	Low	370	no	216.3	M	M	M
TOW21	B747	High	350	no	238.0	M	M	M
USA552	B737-S	High	330	no	261.6	M	M	M
NWA434	B757	High	370	no	216.3	M	M	M
TWA429	B727	Low	310	no	287.0	M	M	M

Table C8. Observations From 1 October 1997

Call Sign	Type	Engine	FL	Observed	Pressure	Temp	In Situ RH	Model RH
COM3921	CL-65	High	330	yes	261.6	-50.8	11	40
AAL1191	MD-80	Low	350	yes	238.0	-53.2	8	70
TWA279	B727	Low	350	yes	238.0	-53.2	8	70
N926TC	HS-25	High	330	no	261.6	-50.8	11	40
TWA519	B727	Low	350	no	238.0	-53.2	8	70
NWA468	DC-9	Low	330	no	261.6	-50.8	11	40
SWG637	DC-9	Low	330	no	261.6	-50.8	11	40
VGD103	B737	High	350	no	238.0	-53.2	8	70
TWA287	B727	Low	350	no	238.0	-53.2	8	70
UPS2076	B747	High	370	no	216.3	-51.9	2	10
COA1125	DC-9	Low	350	no	238.0	-53.2	8	70
N419MB	BE-40	High	390	no	196.5	-50.8	1	10
AWE602	EA-32	High	350	yes	238.0	-53.2	8	70
AJI388	DA-20	High	310	no	287.0	-46.7	14	40
N665MC	C-550	High	310	no	287.0	-46.7	14	40
UPS2062	DC8-S	High	370	yes	216.3	-51.9	2	10
COA516	B737-S	High	370	yes	216.3	-51.9	2	10
N735A	LR-35	High	390	yes	196.5	-50.8	1	10
N235HR	LR-55	High	390	yes	196.5	-50.8	1	10
AAL133	B767	High	390	yes	196.5	-50.8	1	10
ACA829	EA32	High	350	yes	238.0	-53.2	8	70
UAL921	B777	High	390	yes	196.5	-50.8	1	10
COA690	DC-9	Low	330	yes	261.6	-50.8	11	40
UAL977	EA32	High	350	yes	238.0	-53.2	8	70
UPS2134	B757	High	330	yes	261.6	-50.8	11	40
COA449	B737-J	High	350	yes	238.0	-53.2	8	70
NWA440	B757	High	370	yes	216.3	-51.9	2	10
N924EJ	C-750	High	390	yes	196.5	-50.8	1	10
AWE31	EA32	High	350	yes	238.0	-53.2	8	70
AAL199	B767	High	390	yes	196.5	-50.8	1	10
TOW23	B747	High	310	yes	287.0	-46.7	14	40
COA1261	B737-S	High	350	yes	238.0	-53.2	8	70
COA177	B757	High	390	yes	196.5	-50.8	1	10
TWA211	B757	High	390	yes	196.5	-50.8	1	10
N296FA	BE-40	High	370	yes	216.3	-51.9	2	10
USA38	B757	High	370	yes	216.3	-51.9	2	10
DAL491	B757	High	390	yes	196.5	-50.8	1	10

Note: The line between the third and fourth observation delineates between observations taken during the morning and afternoon of 1 October. The observations above and below the line were compared to different forecasts and different soundings.

Table C9. Observations From 2 October 1997

Call Sign	Type	Engine	FL	Observed	Pressure	Temp	In Situ RH	Model RH
NWA1537	DC-9	Low	310	no	287.0	-43.9	51	40
TWA500	MD-80	Low	330	no	261.6	-49.5	43	40
N700KC	CL-60	High	370	yes	216.3	M	M	M
N8270	LR-60	High	390	yes	196.5	M	M	M
NWA434	B757	High	370	yes	216.3	M	M	M
COA1915	B737-S	High	310	no	287.0	-43.9	51	40
NWA444	EA32	High	330	no	261.6	-49.5	43	40
UPS2901	B747	High	330	no	261.6	-49.5	43	40
N77W	HS-25	High	330	no	261.6	-46.6	30	40
N77VJ	LR-24	High	330	no	261.6	-46.6	30	40
DAL342	MD-88	High	330	no	261.6	-46.6	30	40
DAL1094	MD-88	High	330	no	261.6	-46.6	30	40
USA86	B757	High	370	yes	216.3	-57.3	41	40
TWA625	B727	Low	390	yes	196.5	-60.7	38	40
N1191K	BE-30	High	310	no	287.0	-41.1	30	40
NWA426	DC-9	Low	310	no	287.0	-41.1	30	40
SWA1407	B737-S	High	350	yes	238.0	-52.1	48	40
UPS2076	B747	High	370	yes	216.3	-57.3	41	40
AAL133	B767	High	350	yes	238.0	-52.1	48	40
UPS2062	DC8-S	High	370	yes	216.3	-57.3	41	40
COA1261	B737-S	High	350	yes	238.0	-52.1	48	40
AAL173	B767	High	390	yes	196.5	-60.7	38	40
TWA170	MD-80	Low	330	yes	261.6	-46.6	30	40

Note: The line between the eighth and ninth observation delineates between observations taken during the morning and afternoon of 2 October. The observations above and below the line were compared to different forecasts and different soundings.

Table C10. Observations From 4 October 1997

Call Sign	Type	Engine	FL	Observed	Pressure	Temp	In Situ RH	Model RH
TWA417	B757	High	390	no	196.5	-55.3	7	40
UAL9	B767	High	390	no	196.5	-55.3	7	40
EJA923	C-750	High	430	yes	162.3	-61.9	6	40
N2428	BA-10	High	370	no	216.3	-52.5	9	40
UAL95	EA32	High	350	no	238.0	-49.5	11	40
MSR989	B767	High	390	yes	196.5	-55.3	7	40
CCP206	B727	Low	330	no	261.6	-45.7	9	40
N934H	C-650	High	390	no	196.5	-55.3	7	40
UAL11	B767	High	350	no	238.0	-49.5	11	40
UAL609	EA32	High	390	no	196.5	-55.3	7	40

Table C11. Observations From 5 October 1997

Call Sign	Type	Engine	FL	Observed	Pressure	Temp	In Situ RH	Model RH
AAL43	B757	High	350	no	238.0	-44.4	7	40
ACA825	EA-32	High	390	yes	196.5	-53.7	11	40
COM4885	CL65	High	330	no	261.6	-40.0	5	40
AAL1	B767	High	390	yes	196.5	-53.7	11	40

Table C12. Observations From 6 October 1997

Call Sign	Type	Engine	FL	Observed	Pressure	Temp	In Situ RH	Model RH
N766MH	C-650	High	410	yes	178.6	-59.8	16	40
N375SC	DA-22	High	410	yes	178.6	-59.8	16	40
AAL1144	MD-80	Low	370	no	216.3	-51.8	14	40
JOSA591	C-21	High	390	no	196.5	-55.0	12	40
TWA500	MD-80	Low	330	no	261.6	-42.6	14	40
TWA399	B757	High	390	yes	196.5	-55.0	12	40
TWA202	MD-80	Low	370	no	216.3	-51.8	14	40
TWA417	B757	High	410	yes	178.6	-59.8	16	40
ACA825	EA32	High	390	yes	196.5	-55.0	12	40
NWA1110	B757	High	370	no	216.3	-51.8	14	40
AAL1450	MD-80	Low	370	no	216.3	-51.8	14	40
NWA493	DC-9	Low	330	no	261.6	-42.6	14	40
TWA37	B757	High	390	yes	196.5	-55.0	12	40
NWA1473	DC-9	Low	310	no	287.0	-37.2	6	40

Table C13. Observations From 8 October 1997

Call Sign	Type	Engine	FL	Observed	Pressure	Temp	In Situ RH	Model RH
TWA278	DC-9	Low	330	no	261.6	M	M	M
N810GS	HS-25	High	330	no	261.6	M	M	M
UAL55	B757	High	310	no	287.0	M	M	M
TWA287	B727	Low	350	no	238.0	M	M	M
UAL1731	DC-10	High	310	no	287.0	M	M	M
NWA47	B757	High	370	no	216.3	M	M	M
TWA415	DC-9	Low	350	no	238.0	M	M	M
COA641	B737-J	High	350	no	238.0	M	M	M
N944AD	DA-90	High	370	no	216.3	M	M	M
N500LJ	C-500	High	390	no	196.5	M	M	M
NWA799	DC-9	Low	330	no	261.6	M	M	M
N766MH	C-650	High	390	no	196.5	M	M	M
USA166	B737-S	High	330	no	261.6	M	M	M

Table C14. Observations From 9 October 1997

Call Sign	Type	Engine	FL	Observed	Pressure	Temp	In Situ RH	Model RH
TWA296	MD-80	Low	330	no	261.6	M	M	M
USA1202	FK10	High	310	no	287.0	M	M	M
N444CW	C-650	High	350	no	238.0	M	M	M

Table C15. Observations From 10 October 1997

Call Sign	Type	Engine	FL	Observed	Pressure	Temp	In Situ RH	Model RH
N111HZ	C-650	High	390	yes	196.5	-57.1	6	40
N455DW	BE-40	High	410	yes	178.6	-61.1	7	40
N7US	LR-60	High	410	yes	178.6	-61.1	7	40
NWA1110	B757	High	370	no	216.3	-54.5	8	40
TWA192	MD-80	Low	330	no	261.6	-46.3	7	40
NWA476	DC-9	Low	330	no	261.6	-46.3	7	40
NWA1537	DC-9	Low	310	no	287.0	-41.2	7	40
TWA500	MD-80	Low	330	no	261.6	-46.3	7	40
TWA377	MD-80	Low	310	no	287.0	-41.2	7	40
TWA399	B757	High	350	no	238.0	-50.3	7	40
USA1254	DC-9	Low	330	no	261.6	-46.3	7	40
TWA343	MD-80	Low	310	no	287.0	-41.2	7	40
NWA434	B757	High	370	yes	216.3	-54.5	8	40
TWA271	DC-9	Low	350	no	238.0	-50.3	7	40
N96LT	DA-50	High	390	yes	196.5	-57.1	6	40
TWA551	MD-80	Low	310	no	287.0	-41.2	7	40
UAL9	B767	High	350	no	238.0	-50.3	7	40
COA83	B757	High	310	no	287.0	-41.2	7	40
TWA417	B757	High	390	yes	196.5	-57.1	6	40
COA1260	B737-J	High	370	no	216.3	-54.5	8	40
NWA955	B727	Low	330	no	261.6	-46.3	7	40
JOSA715	C-21	High	350	no	238.0	-50.3	7	40
CODY48	C-141	High	310	no	287.0	-41.2	7	40
UAL75	B757	High	310	no	287.0	-41.2	7	40
SWA1001	B737-S	High	310	no	287.0	-41.2	7	40

Table C16. Observations From 12 October 1997

Call Sign	Type	Engine	FL	Observed	Pressure	Temp	In Situ RH	Model RH
NWA243	B727	Low	330	no	261.6	-41.7	51	40
TWA191	MD-80	Low	310	no	287.0	-36.9	31	40
TWA440	B727	Low	370	no	216.3	-50.6	28	40
AAL79	B767	High	350	no	238.0	-47.2	44	40
AAL1770	MD-80	Low	330	no	261.6	-41.7	51	40
NWA996	DC-9	Low	310	no	287.0	-36.9	31	40
TWA98	MD-80	Low	370	no	216.3	-50.6	28	40
NWA1117	DC-9	Low	330	no	261.6	-41.7	51	40
RAX757	LR24	High	390	no	196.5	-53.0	7	40
NWA804	B757	High	370	no	216.3	-50.6	28	40
TWA620	DC-9	Low	330	no	261.6	-41.7	51	40
VGD103	B737	High	310	no	287.0	-36.9	31	40
DAL1094	MD-88	High	330	no	261.6	-41.7	51	40

Table C17. Observations From 13 October 1997

Call Sign	Type	Engine	FL	Observed	Pressure	Temp	In Situ RH	Model RH
COA1668	B737-J	High	370	no	216.3	-49.0	25	40
AWE82	B757	High	350	no	238.0	-45.1	54	40
USA205	DC-9	Low	310	no	287.0	-39.5	36	40
VJA253	DC-9	Low	330	no	261.6	-39.5	46	40
USA623	B737-S	High	310	no	287.0	-39.5	36	40
ACA372	CL-65	High	330	no	261.6	-39.5	46	40
TWA712	B727	Low	370	no	216.3	-49.0	25	40
COA459	B737-J	High	350	no	238.0	-45.1	54	40

Table C18. Observations From 14 October 1997

Call Sign	Type	Engine	FL	Observed	Pressure	Temp	In Situ RH	Model RH
AWE11	B757	High	350	no	238.0	-47.6	22	40
USA552	FK10	High	330	no	261.6	-42.6	36	40
AAL43	B757	High	370	no	216.3	-50.1	8	40
TWA417	B757	High	410	no	178.6	-56.2	4	40
NWA493	DC-9	Low	330	no	261.6	-42.6	36	40
TWA399	B757	High	390	no	196.5	-52.2	4	40
TWA37	B757	High	390	no	196.5	-52.2	4	40
N432QS	G-4	High	430	yes	162.3	-60.3	4	40
TWA500	MD-80	Low	330	no	261.6	-42.6	36	40
TWA123	MD-80	Low	350	no	238.0	-47.6	22	40
USA398	B737	High	330	no	261.6	-42.6	36	40
UAL53	B757	High	350	no	238.0	-47.6	22	40
FDX3609	EA30	High	310	no	287.0	-36.9	32	40
N3123T	BE-40	High	390	no	196.5	-52.2	4	40
NWA489	DC-9	Low	330	no	261.6	-42.6	36	40
COA1264	B737	High	330	no	261.6	-42.6	36	40
N301DM	MU-3	High	350	no	238.0	-47.6	22	40
USA623	B737-S	High	310	no	287.0	-36.9	32	40

Table C19. Observations From 15 October 1997

Call Sign	Type	Engine	FL	Observed	Pressure	Temp	In Situ RH	Model RH
NWA476	DC-9	Low	330	no	261.6	-48.7	12	40
TWA242	DC-9	Low	330	no	261.6	-48.7	12	40
TWA500	MD-80	Low	330	no	261.6	-48.7	12	40
USA1254	DC-9	Low	330	no	261.6	-48.7	12	40
TWA192	MD-80	Low	330	no	261.6	-48.7	12	40
TWA429	B727	Low	310	no	287.0	-46.5	6	40
TWA271	DC-9	Low	350	no	238.0	-51.3	9	70
SMOKY98	C-21	High	410	no	178.6	-53.1	2	10
TWA399	B757	High	370	no	216.3	-51.5	4	10
TWA551	MD-80	Low	350	no	238.0	-51.3	9	70
N901RM	C-560	High	390	no	196.5	-51.0	2	10
NWA493	DC-9	Low	330	no	261.6	-48.7	12	40
TWA417	B757	High	390	yes	196.5	-51.0	2	10
TWA123	MD-80	Low	350	no	238.0	-51.3	9	70
AAL43	B757	High	350	no	238.0	-51.3	9	70
USA398	B737	High	330	no	261.6	-48.7	12	40
TWA377	MD-80	Low	350	no	238.0	-51.3	9	70
N242MT	LR-35	High	410	no	178.6	-53.1	2	10
N54DC	DA-90	High	410	no	178.6	-53.1	2	10
NWA489	DC-9	Low	330	no	261.6	-48.7	12	40
RAX757	LR-25	High	410	no	178.6	-53.1	2	10
UAL11	B767	High	350	no	238.0	-51.3	9	70
N404QS	G-4	High	430	no	162.3	-55.1	1	10
N810D	CL-64	High	390	no	196.5	-51.0	2	10
USA2298	B737	High	330	no	261.6	-48.7	12	40
SWA1001	B737-S	High	310	no	287.0	-46.5	6	40
AWE82	B757	High	350	no	238.0	-51.3	9	70
USA1530	FK-10	High	330	no	261.6	-48.7	12	40
AJI666	LR-24	High	410	no	178.6	-53.1	2	10
VJA253	DC-9	Low	350	no	238.0	-51.3	9	70
N29GD	HS-25	High	370	no	216.3	-51.5	4	10

Table C20. Observations From 16 October 1997

Call Sign	Type	Engine	FL	Observed	Pressure	Temp	In Situ RH	Model RH
UAL445	B757	High	350	yes	238.0	-54.0	21	70
TWA202	MD-80	Low	330	no	261.6	-51.5	26	40
KHA159	DC-9	Low	350	yes	238.0	-54.0	21	70
NWA1110	B757	High	370	yes	216.3	-54.2	10	10
MSR989	B767	High	350	no	238.0	-54.0	21	70
USA167	B737-S	High	310	no	287.0	-47.5	25	40
TWA417	B757	High	390	yes	196.5	-55.3	4	10
NWA476	DC-9	Low	330	no	261.6	-51.5	26	40
TWA377	MD-80	Low	350	no	238.0	-54.0	21	70
TWA551	MD-80	Low	350	no	238.0	-54.0	21	70
EJM92	LR-35	High	410	yes	178.6	-55.4	2	10

Table C21. Observations From 17 October 1997

Call Sign	Type	Engine	FL	Observed	Pressure	Temp	In Situ RH	Model RH
COA1297	B737	High	350	no	238.0	-50.8	3	70
NWA444	EA32	High	330	no	261.6	-49.1	4	40
NWA476	DC-9	Low	330	no	261.6	-49.1	4	40
NWA493	DC-9	Low	330	no	261.6	-49.1	4	40
NWA464	DC-9	Low	330	no	261.6	-49.1	4	40
N880DP	BA11	High	310	no	287.0	-46.8	5	40

Table C22. Observations From 21 October 1997

Call Sign	Type	Engine	FL	Observed	Pressure	Temp	In Situ RH	Model RH
USA742	B737-F	High	370	yes	216.3	-57.0	9	10
NWA287	B757	High	390	yes	196.5	-54.6	6	10
DAL467	B757	High	410	yes	178.6	-52.3	2	10
UAL1229	DC-10	High	350	yes	238.0	-56.6	18	70
TWA279	DC-9	Low	350	yes	238.0	-56.6	18	70
NWA437	B757	High	410	yes	178.6	-52.3	2	10
UAL65	B757	High	350	yes	238.0	-56.6	18	70
UAL10	B767	High	370	yes	216.3	-57.0	9	10
USA24	B757	High	410	yes	178.6	-52.3	2	10
USA44	B757	High	370	yes	216.3	-57.0	9	10

Table C23. Observations From 22 October 1997

Call Sign	Type	Engine	FL	Observed	Pressure	Temp	In Situ RH	Model RH
AAL77	B757	High	390	yes	196.5	-53.3	1	10
N169CA	G-4	High	410	yes	178.6	-53.2	1	10
TOW21	B747	High	350	yes	238.0	-54.4	11	10
AAL33	B767	High	350	yes	238.0	-54.4	11	10
NWA476	DC-9	Low	330	no	261.6	-54.8	16	70
NWA444	EA-32	High	330	yes	261.6	-54.8	16	70
TWA399	B757	High	390	yes	196.5	-53.3	1	10
NWA1821	EA-32	High	350	yes	238.0	-54.4	11	10
AWE11	B757	High	350	yes	238.0	-54.4	11	10
UAL142	B757	High	370	yes	216.3	-52.5	4	10
AAL43	B757	High	350	yes	238.0	-54.4	11	10
TWA5035	B747	High	390	yes	196.5	-53.3	1	10

Table C24. Observations From 28 October 1997

Call Sign	Type	Engine	FL	Observed	Pressure	Temp	In Situ RH	Model RH
USA2128	FK-10	High	310	no	287.0	-48.4	32	40
NWA436	B757	High	370	yes	216.3	-58.4	26	40
N657T	C-650	High	390	yes	196.5	-62.3	21	70
USA718	B737-S	High	330	yes	261.6	-50.1	24	40
USA96	B737-S	High	330	yes	261.6	-50.1	24	40
UAL94	B757	High	370	yes	216.3	-58.4	26	40
TWA8635	DC-9	Low	330	yes	261.6	-50.1	24	40
NWA1522	DC-9	Low	330	yes	261.6	-50.1	24	40
UAL176	B757	High	410	yes	178.6	-62.6	16	10
N945MC	DA01	High	370	yes	216.3	-58.4	26	40
USA89	B757	High	350	yes	238.0	-54.9	30	40
N71MT	HS-25	High	390	yes	196.5	-62.3	21	70
USA21	B757	High	350	yes	238.0	-54.9	30	40
UAL11	B767	High	390	yes	196.5	-62.3	21	70
N43SF	LR-31	High	450	yes	147.4	-63.1	4	10
USA2271	B737-S	High	350	yes	238.0	-54.9	30	40
N191BE	CL-61	High	390	yes	196.5	-62.3	21	70
UAL15	B767	High	350	yes	238.0	-54.9	30	40
AWE25	B757	High	350	yes	238.0	-54.9	30	40

Table C25. Observations From 29 October 1997

Call Sign	Type	Engine	FL	Observed	Pressure	Temp	In Situ RH	Model RH
UAL8150	B767	High	350	yes	238.0	-57.5	19	40
NWA476	B757	High	370	yes	216.3	-61.7	40	40
COA179	B757	High	310	yes	287.0	-48.4	32	40
TWA202	MD-80	Low	370	yes	216.3	-61.7	40	40
UAL976	B767	High	350	yes	238.0	-57.5	19	40
TWA399	B757	High	390	yes	196.5	-66.1	23	70
TWA177	B757	High	410	yes	178.6	-60.0	10	10
TWA675	DC-9	Low	310	yes	287.0	-48.4	32	40
AAL1235	MD-80	Low	350	yes	238.0	-57.5	19	40
N91SA	WW24	High	310	yes	287.0	-48.4	32	40
MEP58	DC-9	Low	350	yes	238.0	-57.5	19	40
COA1706	B737-S	High	330	yes	261.6	-52.7	24	40
SWG621	DC-9	Low	330	yes	261.6	-52.7	24	40
AWE25	B757	High	350	yes	238.0	-57.5	19	40
N508BM	BE-20	High	310	no	287.0	-48.4	32	40
USA88	B757	High	330	yes	261.6	-52.7	24	40
COA278	B737-J	High	370	yes	216.3	-61.7	40	40
NWA436	B757	High	370	yes	216.3	-61.7	40	40
USA800	DC-9	Low	290	yes	314.4	-43.2	31	40
UAL94	B757	High	410	yes	178.6	-60.0	10	10
USA158	B737-F	High	330	yes	261.6	-52.7	24	40
USA718	B737-F	High	290	yes	314.4	-43.2	31	40
NWA494	DC-9	Low	330	yes	261.6	-52.7	24	40
N38AM	LR-35	High	330	yes	261.6	-52.7	24	40
DAL686	B767	High	310	yes	287.0	-48.4	32	40
NWA1522	DC-9	Low	310	yes	287.0	-48.4	32	40
VJA254	DC-9	Low	310	yes	287.0	-48.4	32	40
USA24	B757	High	370	yes	216.3	-61.7	40	40

Table C26. Observations From 30 October 1997

Call Sign	Type	Engine	FL	Observed	Pressure	Temp	In Situ RH	Model RH
TWA37	B757	High	390	yes	196.5	-58.2	10	10
TWA343	MD-80	Low	350	yes	238.0	-56.2	32	40
UAL39	B757	High	390	yes	196.5	-58.2	10	10
KHC289	DA-20	High	350	yes	238.0	-56.2	32	40
NWA490	B727	Low	350	yes	238.0	-56.2	32	40
AAL1	B767	High	390	yes	196.5	-58.2	10	10
N51V	LR-55	High	390	yes	196.5	-58.2	10	10
EJA333	C-560	High	310	yes	287.0	-45.7	30	40
UAL53	B757	High	350	yes	238.0	-56.2	32	40
UAL9	B767	High	390	yes	196.5	-58.2	10	10
AAL1534	MD-80	Low	330	yes	261.6	-51.1	31	40
AAL1806	B757	High	410	yes	178.6	-58.3	4	10
USA938	FK-10	High	350	yes	238.0	-56.2	32	40
N77FK	G-3	High	390	yes	196.5	-58.2	10	10
JERSY04	C-135	High	350	yes	238.0	-56.2	32	40
AWE12	EA32	High	350	yes	238.0	-56.2	32	40
UAL11	B767	High	350	yes	238.0	-56.2	32	40
AAL19	DC-10	High	350	yes	238.0	-56.2	32	40
UAL15	B767	High	350	yes	238.0	-56.2	32	40
USA24	B757	High	370	yes	216.3	-60.2	31	70
AAL3	DC-10	High	310	yes	287.0	-45.7	30	40
USA622	B737-S	High	330	yes	261.6	-51.1	31	40
SWG621	DC-9	Low	330	yes	261.6	-51.1	31	40
N265A	N-265	High	370	yes	216.3	-60.2	31	70
SWG506	DC-9	Low	310	no	287.0	-45.7	30	40
AWE25	B757	High	390	yes	196.5	-58.2	10	10
N731CW	LR-25	High	310	no	287.0	-45.7	30	40
USA44	B757	High	370	yes	216.3	-60.2	31	70
USA88	B757	High	310	yes	287.0	-45.7	30	40
NWA436	B757	High	370	yes	216.3	-60.2	31	70

Note: The line between the eighteenth and nineteenth observation delineates between observations taken during the morning and afternoon of 30 October. The observations above and below the line were compared to different forecasts.

Table C27. Observations From 31 October 1997

Call Sign	Type	Engine	FL	Observed	Pressure	Temp	In Situ RH	Model RH
KHC366	DA-20	High	310	no	287.0	M	M	M
TWA649	MD-80	Low	310	no	287.0	M	M	M
UAL19	B767	High	350	yes	238.0	M	M	M
AAL3	DC-10	High	310	no	287.0	M	M	M
N52DC	DA-50	High	350	yes	238.0	M	M	M
USA24	B757	High	370	yes	216.3	M	M	M
USA44	B757	High	410	yes	178.6	M	M	M
N40PH	C-650	High	410	yes	178.6	M	M	M
N945CE	HS-25	High	350	yes	238.0	M	M	M
USA88	B757	High	330	no	261.6	M	M	M

Bibliography

Air Weather Service (AWS), 1953: A Further Analysis of Contrail Data, Air Weather Service Tech. Rep. AWS/TR-105-112, HQ Air Weather Service, 40 pp.

Air Weather Service (AWS), 1979: The Use of the Skew-T, Log-P Diagram in Analysis and Forecasting, Air Weather Service Tech. Rep. AWS/TR-79/006, HQ Air Weather Service, 140 pp.

Air Weather Service (AWS), 1981: Forecasting Aircraft Condensation Trails, Air Weather Service Tech. Rep. AWS/TR-81/001, HQ Air Weather Service, 46 pp.

Analytical Software, 1996: STATISTIX® for Windows Users Manual, 333 pp.

Appleman, Herbert S., 1953: The Formation of Exhaust Condensation Trails by Jet Aircraft, *Bull. Amer. Meteor. Soc.*, **34**, 14-20.

Appleman, Herbert S., 1957: Derivation of Jet-Aircraft Contrail-Formation Curves, Air Weather Service Tech. Rep. AWS/TR 105-145, HQ Air Weather Service, 46 pp.

Asbury, Robert P. III, 1997: An Examination of the Hanson Contrail Forecast Algorithm Under Low Relative Humidity Conditions, 101 pp.

Aviation Supplies and Academics (ASA), 1990: Federal Aviation Regulations (FAR), FAR Part 71 - Designation of Federal Airways, Area Low Routes, Controlled Airspace, and Reporting Points, Federal Aviation Administration, 7 pp.

Aviation Supplies and Academics (ASA), 1990: Federal Aviation Regulations (FAR), FAR Part 91 - General Operating and Flight Rules, Federal Aviation Administration, 77 pp.

Aviation Supplies and Academics (ASA), 1990: Airman's Information Manual (AIM), Basic Flight Information and ATC Procedures, 382 pp.

Bjornson, Brian. M., 1992: SAC Contrail Formation Study, USAF Environmental Technical Applications Center Project Rep. USAFETAC/PR-92/003, 48 pp.

Coleman, Rich F., 1996: A New Formulation for the Critical Temperature for Contrail Formation, *J. Appl. Meteor.*, **35**, 2270-2282. (December 1996).

Devore, Jay L., 1995: Probability and Statistics for the Engineering and Sciences, 4th Edition, Duxbury Press, 467 pp.

Hanson, Harvey M. And Douglas M. Hanson, 1995: A Reexamination of the Formation of Exhaust Condensation Trails by Jet Aircraft", *J. Appl. Meteor.*, **34**, 2400-2405. (December 1995).

Jiusto, James E., 1961: Prediction of Aircraft Condensation Trails, PROJECT CONTRAILS, Cornell Aeronautical Laboratory Report No. VC-1055-P-5, 26 pp.

Jiusto, J. E., and R. J. Pilie, 1958: A Laboratory Study of Contrails, *J. Meteor.*, **15**, 149-154.

Jiusto, James E., and R. J. Pilie, 1964: Contrail Forecasting, Cornell Aeronautical Laboratory Report No. VC-1660-P-3, 33 pp.

Lambert, Mark and Kenneth Munson, 1994: Jane's All the World's Aircraft 1994-1995, Butler and Tanner Ltd., 748 pp.

Laracuente, Israel, 1997: Weather Displays and Applications Branch, Air Force Global Weather Center, Offutt Air Force Base, NE. Personal Communication.

MathSoft, 1995: User's Guide, MATHCAD PLUS 6.0, MathSoft, Inc., 694 pp.

Miller, Walter F., 1990: SAC Contrail Forecasting Algorithm Validation Study, USAF Environmental Technical Applications Center Project Rep. USAFETAC/PR-90/003, 28 pp.

Minnis, Patrick, J. Kirk Ayers, and Steven P. Weaver, 1997: Surface-Based Observations of Contrail Occurrence Frequency Over the U.S., April 1993 - April 1994, NASA Reference Publication 1404, 31 pp.

NASA Ames Research Center, 1996: SUbsonic aircraft: Contrail and Cloud Effects Special Study (SUCCESS), Mission Plan, Ames Research Center, 99 pp.

Peters, Jeffrey L., 1993: New Techniques for Contrail Forecasting, Air Weather Service Tech. Rep. AWS/TR-93/001, HQ Air Weather Service, 35 pp.

Polander, John F., 1997: Aeronautical Systems Meteorologist, 88th Weather Squadron, Wright-Patterson Air Force Base, OH. Personal Communication.

Rabayda, Allen C., 1997: Moisture Sensitivity of Contrail Forecast Algorithms, 108 pp.

Reynolds, Daniel E., 1997: Assistant Professor of Statistics, Air Force Institute of Technology, Wright-Patterson Air Force Base, OH. Personal Communication.

Rogers, R. R. and M. K. Yau, 1994: A Short Course in Cloud Physics, Butterworth Heinemann, 290 pp.

Saatzer, P., 1995: Pilot Alert System Flight Test: Final Technical Report for Period November 1998 - May 1993, B-2 Division, Northrop Grumman Corporation, 241 pp.

Sassen, Kenneth, 1997: Contrail Cirrus and their Potential for Regional Climate Change, *Bull. Amer. Meteor. Soc.*, **78**, 1885-1903. (September 1997)

Sausen, Robert, Klaus Gierens, and Ulrich Schumann, 1997: A Diagnostic Study of the Global Coverage by Contrails, Deutsche Forschungsanstalt fur Luft und Raumfahrt, Institut fur Physik der Atmosphare, Report No. 89, 21 pp.

Schrader, Mark L., 1994: Calculations of Critical Temperature of Contrail Formation for Different Engine Types (Draft), HQ Air Weather Service, 15 pp.

Schumann, Ulrich, 1996: On Conditions for Contrail Formation from Aircraft Exhausts, *Meteorologisch Zeitschrift*, N.F.**5**, 4-23. (February 1996).

Schumann, Ulrich, 1996: Comments on "A Reexamination of the Formation of Exhaust Condensation Trails by Jet Aircraft", *J. Appl. Meteor.*, **35**, 2283-2284. (December 1996).

Slattery, DeEtte R., 1998: Chief Controller, Air Traffic Control Tower, 88th Operations Support Squadron, Wright-Patterson Air Force Base, OH. Personal Communication.

Speltz, David J., 1995: Validation of the Appleman Contrail Forecasting Scheme Using Engine Specific Aircraft Data. Cloud Impacts on DoD Operations and Systems, 1995 Conference (CIDOS-95), Hanscom Air Force Base, MA.

Vaisala Promotional Package, 1996: RS80 Radiosonde, Vaisala, Inc. Helsinki, Finland.

Wallace, John M., and Peter V. Hobbs, 1997: Atmospheric Science: An Introductory Survey, Academic Press, 467 pp.

Weaver, Steven P., 1997: Chief Aeronautical Systems Meteorologist, 88th Weather Squadron, Wright-Patterson Air Force Base, OH. Personal Communication.

Wilks, Daniel S., 1995: Statistical Methods in the Atmospheric Sciences, Academic Press, 467 pp.

Vita

Jeffrey David Shull was born on 7 September 1969 in Newark, Ohio. After graduating from Newark High School in 1987 he enrolled in The Ohio State University College of Engineering and the Air Force Reserve Officer Training Corps program. He was commissioned a Second Lieutenant upon his graduation with a degree in Aviation Engineering with a Concentration in Atmospheric Science in 1991.

Captain Shull's active duty first assignment was to attend the Basic Meteorology Program at Florida State University in 1992. Upon receipt of a Certificate in Meteorology in 1993 he was assigned to Headquarters, Air Combat Command (ACC) at Langley Air Force Base, Virginia, where he served as a weather officer at the ACC Weather Support Unit. His duties there included issuing mission control forecasts for worldwide aircraft deployments, providing weather briefings to the ACC commander and staff, and flying aboard Airborne Deployment Control Aircraft while serving in the capacity of Airborne Mission Control Team Staff Weather Officer. In 1995 he was assigned to the 1st Operations Support Squadron as the commander of the weather flight, and he was promoted to his current rank of Captain in December of the same year. Captain Shull deployed with the 1st Fighter Wing to Azraq, Jordan in April 1996 in support of the second Airpower Expeditionary Force (AEF II). He entered the Meteorology program at the Air Force Institute of Technology in September 1996 and graduated with a Master of Science degree in Meteorology on 24 March 1998. He was then assigned to the 88th

Weather Squadron at Wright-Patterson Air Force Base where he expects to serve as a Staff Meteorologist in 1998, 1999, and 2000.

Captain Shull has two children; Cassandra, born in 1991, and Zachary, born in 1992.

Permanent Address: 1855 Londondale Parkway
Newark, OH 43055

REPORT DOCUMENTATION PAGE

Form Approved OMB No. 0704-0188

Public reporting burden for this collection of information is estimated to average 1 hour per response, including the time for reviewing instructions, searching existing data sources, gathering and maintaining the data needed, and completing and reviewing the collection of information. Send comments regarding this burden estimate or any other aspect of this collection of information, including suggestions for reducing this burden, to Washington Headquarters Services, Directorate for Information Operations and Reports, 1215 Jefferson Davis Highway, Suite 1204, Arlington, VA 22202-4302, and to the Office of Management and Budget, Paperwork Reduction Project (0704-0188), Washington, DC 20503.

1. AGENCY USE ONLY *(Leave blank)*	2. REPORT DATE	3. REPORT TYPE AND DATES COVERED
	March 1998	Final

4. TITLE AND SUBTITLE
A Validation Study of the Air Force Weather Agency (AFWA) JETRAX Contrail Forecast Algorithm

5. FUNDING NUMBERS

6. AUTHOR(S)
Jeffrey D. Shull, Capt, USAF

7. PERFORMING ORGANIZATION NAME(S) AND ADDRESS(ES)
AFIT/ENP
2950 P Street
Wright-Patterson AFB, OH 45433
Attn: Lt Col Michael K. Walters, COMM: (937) 255-3636 x4681
e-mail: mwalters@afit.af.mil

8. PERFORMING ORGANIZATION REPORT NUMBER
AFIT/GM/ENP/98M-10

9. SPONSORING/MONITORING AGENCY NAME(S) AND ADDRESS(ES)
88 WS
2049 Monahan Way, Bldg 91
Wright-Patterson AFB, OH 45433
Attn: Mr. Steve Weaver, COMM (937) 255-2207
e-mail: weaversp@88abw.wpafb.af.mil

10. SPONSORING/MONITORING AGENCY REPORT NUMBER

11. SUPPLEMENTARY NOTES

12a. DISTRIBUTION AVAILABILITY STATEMENT
Approved for Public Release; Distribution Unlimited

12b. DISTRIBUTION CODE

13. ABSTRACT *(Maximum 200 words)*

Accurate contrail forecasts allow pilots to avoid levels of the atmosphere which are conducive to contrail formation, reducing their likelihood of being visually detected by enemy forces. The primary objective of this thesis was to evaluate the performance of the JETRAX contrail forecast algorithm currently used by the Air Force Weather Agency to support military air operations.

A total of 397 ground based contrail observations were collected at Wright-Patterson Air Force Base on 27 different days. Observations were collected with the aid of air traffic control radar, which greatly facilitated the positive identification of overflying aircraft and provided necessary information such as aircraft type and flight level. This data set was used to validate corresponding contrail forecasts disseminated to operational users via the Air Force Weather Information Network (AFWIN).

All forecast products derived from the JETRAX algorithm demonstrated greater skill than persistence, climatology, or other algorithms tested with real time radiosonde data. An 84.4 percent accuracy rate was observed. Based on this research, the Air Force Weather Agency is providing excellent contrail forecasts to their operational users, and while there is still room for improvement, no immediate changes to the JETRAX algorithm are warranted.

14. SUBJECT TERMS
Meteorology, Contrails, Condensation Trails, JETRAX, Air Force Weather Agency Contrail Forecast Algorithm

15. NUMBER OF PAGES
138

16. PRICE CODE

17. SECURITY CLASSIFICATION OF REPORT	18. SECURITY CLASSIFICATION OF THIS PAGE	19. SECURITY CLASSIFICATION OF ABSTRACT	20. LIMITATION OF ABSTRACT
Unclassified	Unclassified	Unclassified	UL